DOKUZ EYLÜL UNIVERSITY

GRADUATE SCHOOL OF NATURAL AND APPLIED SCIENCES

INVESTIGATION OF THERMAL BEHAVIORS OF NANO PARTICLE-BASED PHASE CHANGE MATERIALS

by

Şeyma İNCE

December, 2014

İZMİR

INVESTIGATION OF THERMAL BEHAVIORS OF NANO PARTICLE-BASED PHASE CHANGE MATERIALS

A Thesis Submitted to the
Graduate School of Natural and Applied Sciences of Dokuz Eylül University In
Partial Fulfillment of the Requirements for the Degree of Master of Chemistry
Program

by
Şeyma İNCE

December, 2014
İZMİR

M.Sc THESIS EXAMINATION RESULT FORM

We have read the thesis entitled **"INVESTIGATION OF THERMAL BEHAVIORS OF NANO PARTICLE-BASED PHASE CHANGE MATERIALS"** completed by **ŞEYMA İNCE** under supervision of **ASSOC. PROF. DR. YOLDAŞ SEKİ** and we certify that in our opinion it is fully adequate, in scope and in quality, as a thesis for the degree of Master of Science.

Assoc. Prof. Dr. Yoldaş SEKİ

Supervisor

Prof. Dr. Mehmet Kadir YURDAKOÇ

(Jury Member)

Assist. Prof. Dr. M. Akif EZAN

(Jury Member)

Prof.Dr. Ayşe OKUR
Director
Graduate School of Natural and Applied Sciences

ACKNOWLEDGMENTS

INVESTIGATION OF THERMAL BEHAVIORS OF NANO PARTICLE-BASED PHASE CHANGE MATERIALS

ABSTRACT

In this study, thermal conductivities of Arachidic acid (AA) and Myristic acid (MA) is aimed to be increased by loading graphite nanoplates (GNP) with various fractions, namely 0.5, 1, 2- percent. Melting and freezing temperatures, latent heats of melting and freezing, the extent of supercooling and the extent of crystallinity were obtained in terms of the GNP loadings. The effect of GNP loading on thermal stability and functional groups of AA and MA were determined by thermo gravimetric analysis (TGA) and Fourier transform infrared (FTIR), respectively.

The thermal cycling tests showed that the composite phase change materials (PCMs) had good thermal reliability and chemical stability, after 100 melting and freezing cycling. TGA results of the composite PCMs indicated that the composite PCMs had good thermal durability above their working temperature ranges. Thermal conductivity of the AA has been increased by 15, 30 and 43-percent whereas for MA, conductivity has been increased by 8, 18 and 38-percent after the GNP loading for 0.5, 1 and 2-percent, respectively.

Results reveal that while the GNP loading does not cause any major change on the phase change temperature and the latent heat values even for the long term utilization, significant increment on the thermal conductivity is achieved. It is also evaluated that the degree of sub-cooling decreases with increasing the GNP fraction.

Keywords: Phase change materials (PCMs), thermal properties, Arachidic acid, Myristic acid, thermal conductivity, latent heat.

NANO PARÇACIK ESASLI FAZ DEĞİŞİM MALZEMELERİNİN TERMAL DAVRANIŞLARININ İNCELENMESİ

ÖZ

Bu çalışmada Araşidik asit (AA) ve Miristik asit (MA) numunelerine yüzde 0,5; 1 ve 2 gibi farklı kütlesel oranlarda grafit nano-tabakalar (GNT) eklenerek malzemelerin termal iletkenliğinin arttırılması amaçlanmıştır. Malzemelerin erime ve katılaşma sıcaklıkları, erime ve donma gizli ısıları, aşırı soğuma dereceleri ve kristallik derecesi grafit nano tabakalar yüklemesi bakımından elde edilmiştir. GNT yüklemesinin AA ve MA numunelerinin termal kararlılık ve fonksiyonel grupları üzerine etkisi, TGA ve FTIR cihazları ile incelenmiştir.

Termal çevrim testleri sonucunda, kompozit faz değişim malzemelerinin (FDM) 100 defa eritilip dondurulmasına rağmen iyi bir termal güvenirliliğe ve kimyasal kararlılığa sahip olduğu anlaşılmıştır. TGA sonuçları ile kompozit malzemelerinin kendi çalışma sıcaklıklarının üzerinde iyi bir termal dayanıklılık gösterdikleri görülmüştür. Yüzde 0,5; 1 ve 2 GNT yüklemesinden sonra, AA faz değişim malzemesinin termal iletkenliği sırasıyla, yüzde 15, 30 ve 43, MA faz değişim malzemesinin ise yüzde 8, 18 ve 38 oranlarında arttırılmıştır.

Sonuçlar GNT yüklemesinin kompozit FDM'lerin faz değişim sıcaklıklarında ve gizli ısı değerlerinde önemli bir değişikliğe neden olmazken, uzun süreli kullanımlarda termal iletkenlik üzerinde önemli bir artış elde edilebilir olduğunu göstermektedir. Buna ek olarak, GNT katkı oranının arttırılmasıyla aşırı soğuma derecesinin azaldığı görülmektedir.

Anahtar kelimeler: Faz değişim malzemeleri (FDM), termal özellikler, araşidik asit, miristik asit, termal iletkenlik, gizli ısı.

CONTENTS

LIST OF FIGURES

LIST OF TABLES

CHAPTER ONE
INTRODUCTION

1.1 General Introduction

Sustainability of renewable energy resources is a big problem for using the environmental friendly sources in industrial or domestic applications with rapid economic development, energy deficit, and environmental problems in the world. Thermal energy storage (TES) is a key technology in reducing the mismatch between energy supply and demand for heating and cooling systems and TES upgrades performance and dependability of energy systems (Dincer & Rosen, 2002). Thermal energy storage methods can be explained as storage of the heat or cold energy while the energy sources are widely available (daytime), and the stored energy can be discharged when the sources are limited. Energy can be stored as a change in internal energy of a material as a latent heat, sensible heat and thermo chemical or combination of them (Sharma, Tyagi, Chen & Buddhi, 2009).

Two types of TES techniques are commonly in use for heating or cooling applications; *sensible heat TES* and *latent heat TES*. Sensible heat systems utilize the heat capacity and the change in temperature of material during the process of charging and discharging, whereas the latent heat systems, energy storage occurs via changing the phase of the material at constant temperature, by melting or freezing. In the following section basics of the TES systems are briefly introduced.

1.1.1 Sensible Thermal Energy Storage (STES)

When the temperature of storage medium increases *(heating)* or decreases (cooling), a material is stored as sensible heat, as seen in Figure 1.1 The amount of heat that can be stored depends on heat capacity of the medium, the amount of change in temperature and the amount of the storage medium. In the sensible heat storage systems, it is desirable for the storage medium to have high specific heat

capacity, stability under thermal cycling, availability and most importantly inexpensive (Hasnain, 1998).
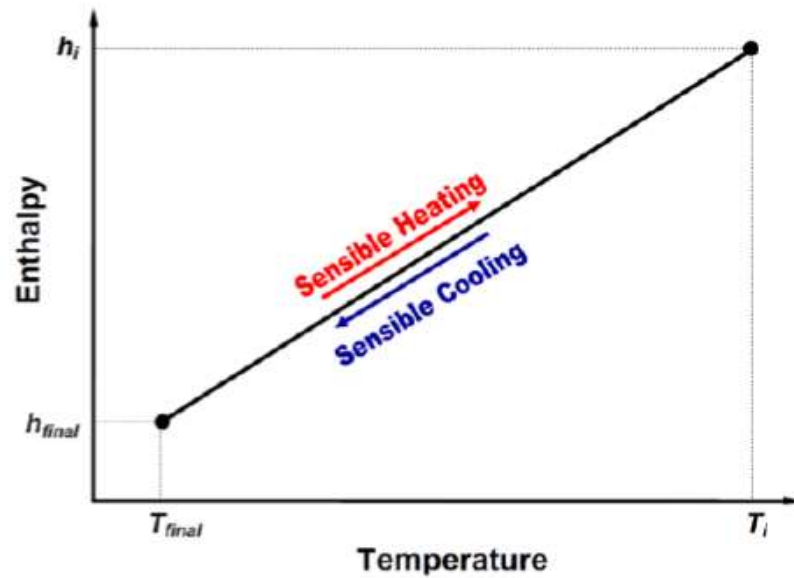
Figure 1.1 Enthalpy-temperature variation of sensible heat storage (Ezan, 2011)

Solid or *liquid* materials can be selected as storage medium in sensible energy storage systems. Sharma et al. (2009) and Hasnain (1998) emphasized that water is the best sensible heat storage (SHS) liquid among the storage materials because it is inexpensive and has a high specific heat. However, many materials can be used for sensible heat storage such as oils, molten salts, liquid metals, etc. The total energy variation of a sensible heat storage system can be defined as,

$$\Delta E = \int_{T_l}^{T_f} (mc)dT = (mc)\left[T_f - T_i\right] \tag{1.1}$$

1.1.2 Latent Thermal Energy Storage (LTES)

Latent heat storage is based on heat storage or release when a storage medium undergoes a phase change from the solid to liquid or liquid to gas, or vice versa (Sharma et al., 2009). As an instance heating and cooling process of a substance, i.e. phase change material, is illustrated in Figure 1.2. At first, in this process, temperature of the PCM decreases (release heat) as in the sensible heat storage

systems. Afterwards, as the temperature of PCM reaches to its phase change temperature (T_m), phase change process initiates and latent heat is stored during the phase change process. As a result, energy storage takes place at a constant temperature unlike sensible heat storage. When the storage medium changes phase from solid to liquid or from liquid to solid, the corresponding storage materials are referred to phase change materials (PCMs) (Ezan, 2011).
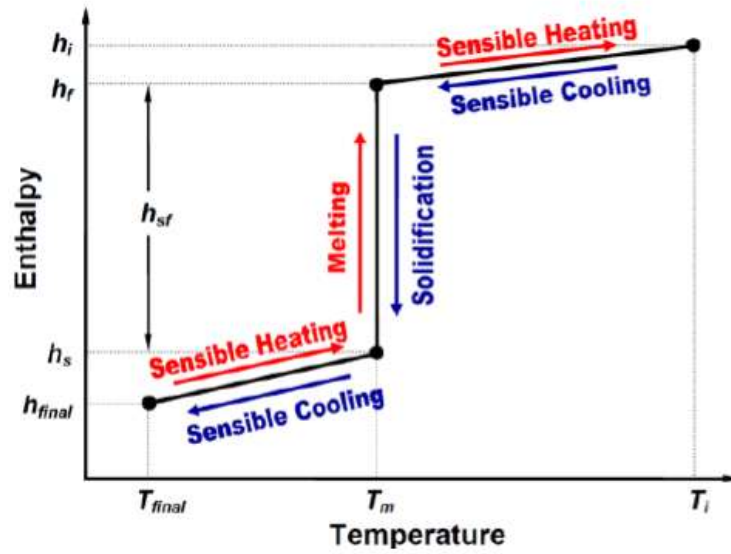
Figure 1.2 Enthalpy-temperature variation of latent heat storage (Ezan, 2011)

The total heat storage capacity of a latent heat storage system with liquid–solid phase transformation can be defined as follows,

$$\Delta E = (mc)_l \left[T_m - T_i \right] + m h_{sf} + (mc)_s \left[T_{final} - T_m \right] \tag{1.2}$$

Latent heat storage provides much higher energy storage density with smaller temperature fluctuations when compared with the sensible heat storage method. Solid-liquid PCMs are more convenient than other phase transformations. Because relatively large amount of heat can be stored in PCMs over a narrow temperature range, without high volume change (Hasnain, 1998).

1.2 Phase Change Materials

Many materials are used in latent energy storage systems. The latent heat storage materials are commonly known as phase change materials (PCMs). Many studies of phase change materials were made by researches for the latent energy storage systems (Abhat, 1983; Farid et al., 2004; Sharma et al., 2009; Zalba, et al., 2003). According to these researchers, PCMs should have some significant properties to be beneficial in the latent heat storage systems. Sharma et al. (2009) briefly explained the main properties of PCMs as given in Table 1.1.

Table 1.1 Characteristics of PCMs. (Sharma et al., 2009)

Thermal Properties	Kinetic or Physical Properties	Chemical Properties	Economic Factors
(1) Suitable phase change temperature range,	(5) No subcooling,	(10) Long-term chemical stability,	(15) Abundant,
(2) High latent heat of transition,	(6) High density,	(11) No toxicity,	(16) Available,
(3) High specific heat,	(7) Small volume change,	(12) Non-flammable,	(17) Cheap,
(4) Large thermal conductivity in both solid and liquid phases,	(8) Low vapour pressure,	(13) Compatibility with construction and container materials,	
	(9) Sufficient crystallization rate,	(14) Completely reversible phase change,	

Several authors have presented useful classifications of PCMs which may be used for thermal energy storage. The available classification of different materials that can be used as PCM are presented in the Figure 1.3 and their melting temperature and enthalpy range are presented in Figure 1.4
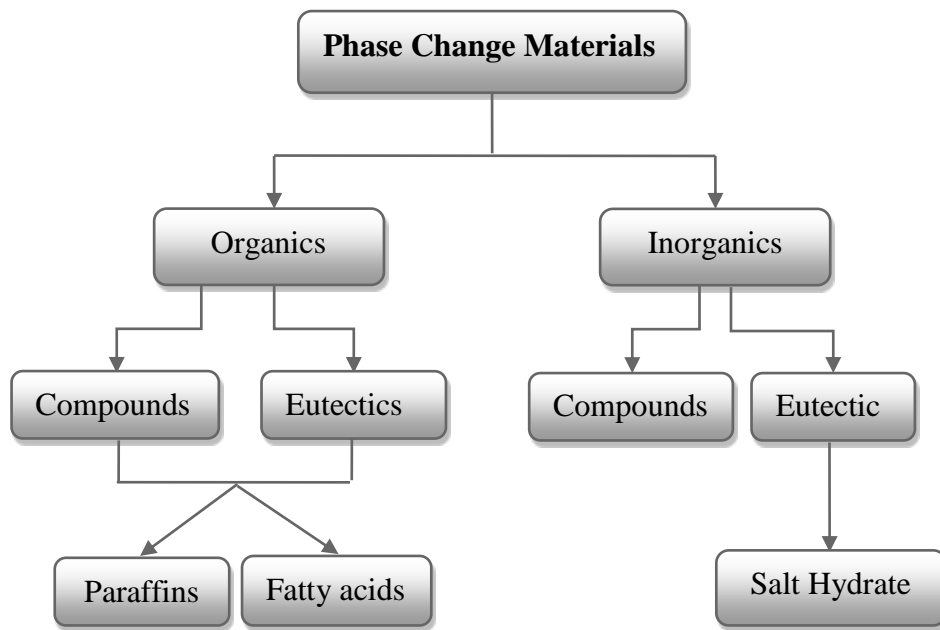
Figure 1.3 Variety of phase change heat storage materials (Oró et al., 2012)
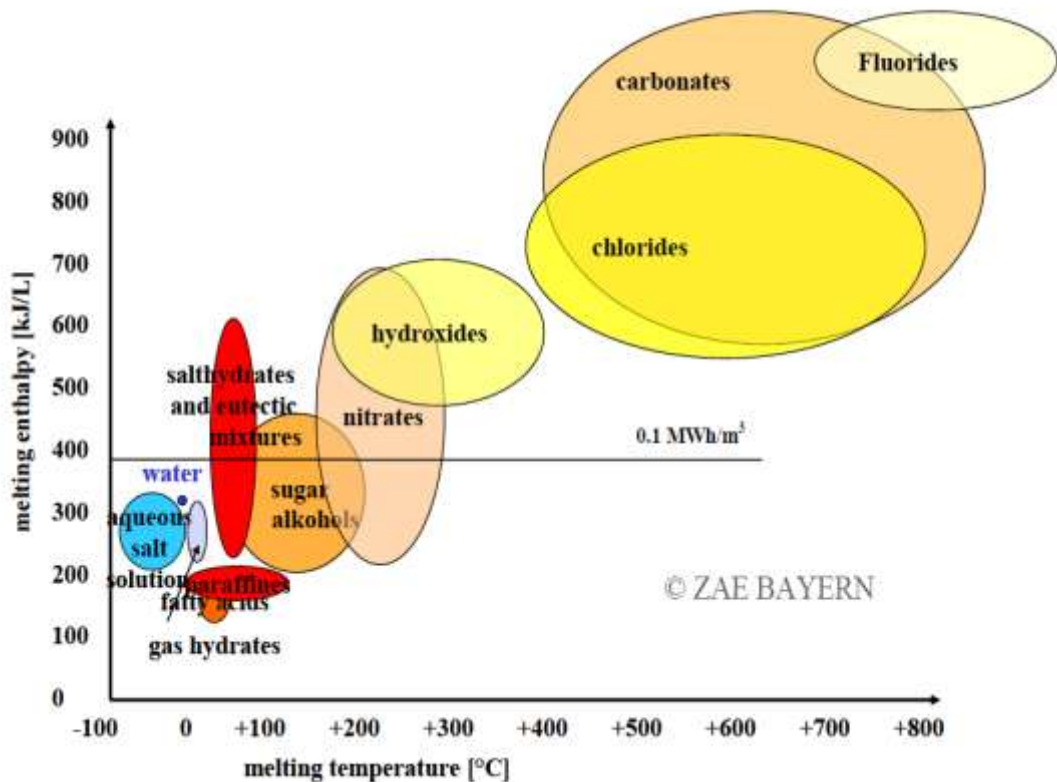
Figure 1.4 Classes of materials that can be used as PCM with their typical melting temperature and enthalpy (Mehling and Cabeza, 2008)

1.2.1 Paraffins

The most widely used organic PCM is paraffins in storage medium. Paraffins are technically called as alcane and general chemical formula is shown in Figure 1.5 expressed as C_nH_{2n+2}.

$$H \;-\; \underset{\underset{H}{|}}{\overset{\overset{}{|}}{C}} \;-\; \underset{\underset{}{|}}{\overset{\overset{}{|}}{C}} \;-\; ... \;-\; \underset{\underset{H}{|}}{\overset{\overset{H}{|}}{C}} \;-\; \underset{\underset{H}{|}}{\overset{\overset{H}{|}}{C}} \;-\; H$$
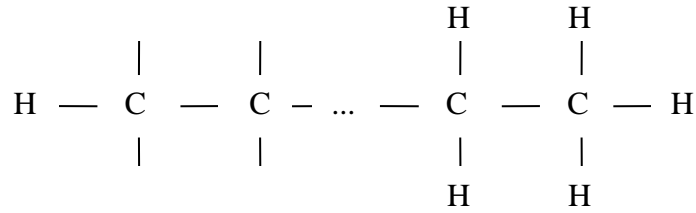
Figure 1.5 Chemical structure of alcane

Paraffins demonstrate many good features in terms of thermal energy storage. For instance; having high phase change enthalpy, little or no subcooling, low vapour pressure in the melting state, chemically and thermally stable, no phase separation and commercial availability. Paraffin waxes are safe and non-reactive. But paraffins have several undesirable features besides the good properties. These are; low thermal conductivity, high volume change during phase change and flammable (depending on containment).

As shown in some studies, adding high thermal conductivity materials is provided to increase thermal conductivity of the phase change materials. According to researchers metallic fillers, metal matrix structures, finned tube and aluminium shavings may be used to improve their thermal conductivity (Fan & Khodadadi, 2011; Hasnain, 1998). In order to solve the problem of the high density during the phase change different geometry types and capsules are used.

1.2.2 Salt Hydrates

Salt hydrates are the most important material of PCMs, and have temperature range of 5 to 130°. They consist of a salt and water. Salt hydrates are charming materials for use in thermal energy storage due to their high volumetric storage

6

density and comparatively high thermal conductivity. This can increase heat transfer in and out of the storage unit. They have a sharp melting point and a high heat of fusion when compared with other heat storage PCMs. On the other hand, they have some disadvantages properties, such as phase separation and sub-cooling. The biggest problem caused by freezing and thawing cycle is phase separation (Karathia, 2011).

Phase separation is a state where components with the different densities of a material settle down in a stratified pattern according to ascending density values (Mehling and Cabeza, 2008). To reduce this problem, it can be used gelled and thickened mixtures (Sharma et al., 2005). Phase separation of a salt hydrate can be seen in the Figure 1.6.

Figure 1.6 Phase separation of a salt hydrates (Streicher, Cabeza and Heinz, 2005)

Subcooling is another problem associated with salt hydrates. When the temperature of a liquid is decreased below its melting temperature, material may not solidified. This event referred to *subcooling* or *supercooling*. In Figure 1.7 subcooling effect is indicated on the temperature-time diagram.
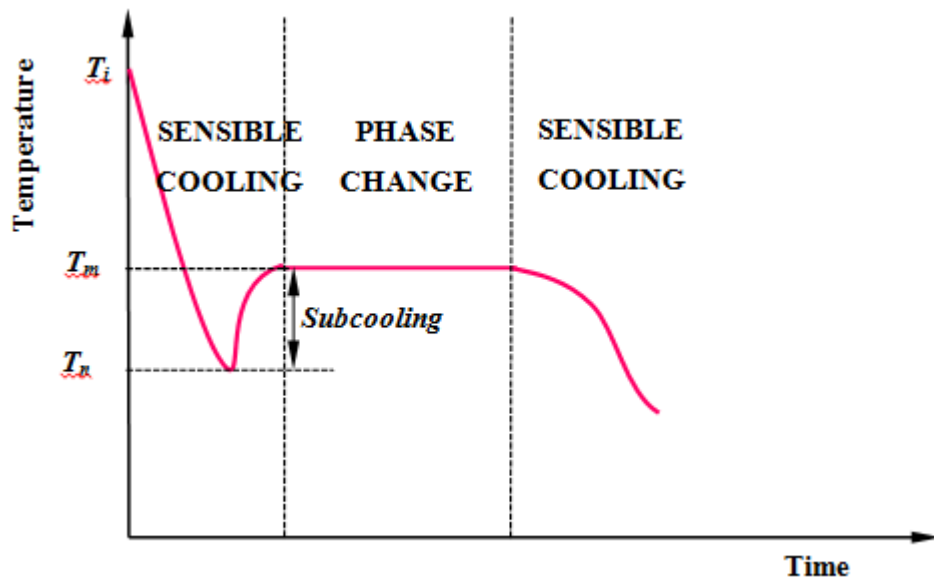
Figure 1.7 Effect of the subcooling

Although (T_i) material in the initial temperature reaches to its (T_m) melting temperature at the end of the sensible cooling process, nucleation does not occur. When the temperature of material reaches to the critical temperature (T_n) with continued cooling process, nucleation (solidification) occurs. The first occurrence of nucleation temperature is defined as nucleation temperature T_n. Rapidly temperature of the material increases and reaches its melting temperature with the start of nucleation and phase change process occurs at this temperature. The difference between melting temperature and nucleation temperature $(\Delta T = T_m - T_n)$ is named subcooling degree. This impact is undesirable status because it extends the operating temperature range of the phase change materials. Subcooling can be avoided using suitable nucleating materials and thickening agent to start crystal growth in the storage media. These additives are materials with similar crystal structure as the solid PCM. Different suggestions to get rid of subcooling on the level of the PCM are mentioned by researchers (Farid, Khudhair, Razack & Al–Hallaj, 2004; Huang et al., 2010; Sharma & Sagara, 2005; Mehling and Cabeza, 2008).

1.2.3 Eutectic Mixtures

Eutectic materials occur with mixtures of two or more compounds. They have congruent melting and freezing when mixed in a proper proportion during the storage process. Eutectic mixtures almost always melt and freeze without segregation, leaving little opportunity for the components to separate (Oró et al. 2012). They melt nearly at constant temperature. Salts, salt hydrates, aqueous solutions and water are main inorganic materials for phase change materials. Eutectic materials indicate some advantages. For instance, similar thermal conductivity as water and having good energy storage density. Furthermore, besides the good properties they have several disadvantages. They show subcooling and they present phase separation because of the stratification of the salt and the water. Sharma et al. (2009) shortly summarized list of developed inorganic and organic eutectic mixtures with potential use as PCM are shown in Table 1.2.

Table 1.2 Inorganic and organic eutectic mixture with potential use as PCM   (Sharma et al., 2009)

Material	Composition (wt.%)	Melting point (^{o}C)	Latent heat (kJ/kg)
$CaCl_2.6H2O + CaBr_2.6H2O$	45 + 55	14.7	140
Triethylolethane + water + urea	38.5 + 31.5 + 30	13.4	160
$C_{14}H_2.8O_2 + C_{10}H_{20}O_2$	34 + 66	24	147.7
$CaCl_2 + MgCl_2.6H_2O$	50 + 50	25	95
$CH_3CONH_2 + NH_2CONH_2$	50 + 50	27	163
Triethylolethane + urea	62.5 + 37.5	29.8	218
$Ca(NO_3)4H_2O + Mg(NO_3)_3.6H2O$	47 + 53	30	136
$CH_3COONa.3H_2O + NH_2CONH_2$	40 + 60	30	200.5
$NH_2CONH_2 + NH_4NO_3$	53 + 47	46	95
$Mg(NO_3)_3.6H_2O + NH_4NO_3$	61.5 + 38.5	52	125.5
$Mg(NO_3)_3.6H_2O + MgCl_2.6H_2O$	58.7 + 41.3	59	132.2
$Mg(NO_3)_3.6H_2O + MgCl_26H_2O$	50 + 50	59.1	144
$Mg(NO_3)_3.6H_2O + Al(NO_3)_2.9H_2O$	53 + 47	61	148
$CH_3CONH_2 + C_{17}H_{35}COOH$	50 + 50	65	218
$Mg(NO_3)_2.6H_2O + MgBr_2.6H_2O$	59 + 41	66	168
Napthalene + benzoic acid	67.1 + 32.9	67	123.4
$NH_2CONH_2 + NH_4Br$	66.6 + 33.4	76	151
$LiNO_3 + NH_4NO_3 + NaNO_3$	25 + 65 + 10	80.5	113
$LiNO_3 + NH_4NO_3 + KNO_3$	26.4 + 58.7 + 14.9	81.5	116
$LiNO_3 + NH_4NO_3 + NH_4Cl$	27 + 68 + 5	81.6	108

1.2.4 Fatty acids

Fatty acids are organic compounds and are formulated as CH_3-$(CH_2)_{2n}$.$COOH$. In other words fatty acids have long unbranched aliphatic chains and they also called as carboxylic acids. They have same characteristics as paraffins. Chemical structure of fatty acids is shown in Figure 1.8.
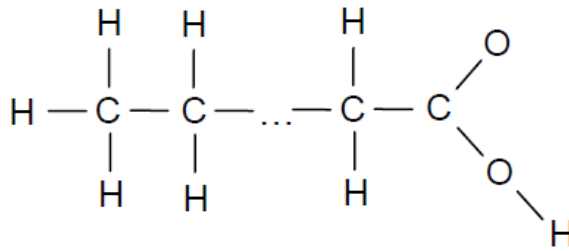
Figure 1.8 Chemical structure of fatty acids

As shown in the Figure 1.8, one end of the molecule ends with a –COOH instead of a –CH_3 group in contrast to a paraffin structure. Some properties of the fatty acids are similar to that of paraffins. For instance, melting enthalpies of paraffins and fatty acids show similar characteristics. The melting temperature of fatty acids depends on the length of the molecule. Namely, if the length of the molecule increases, melting temperature of fatty acids also rises.

From the point of view thermo-pyhsical properties, fatty acids have relatively high latent heat values compared with paraffins. They also have good repeatability, congruent freezing and melting points, no phase segregation, no or little subcooling and low thermal conductivity. The melting temperatures of fatty acids vary from -5 $^{\circ}$C to 71 $^{\circ}$C and their latent heat values are in the range of 45 kJ/kg - 210 kJ/kg (Kenisarin & Mahkamov, 2007). As a result, they can be called as good phase change material candidates. Some fatty acids that can be used as PCMs are listed in Table 1.3 (Sharma & Sagara, 2005; Mehling and Cabeza, 2008; Farid et al., 2004; Abhat, 1983).

Table 1.3 Physical properties of some fatty acids

Compound	Melting temp.(^{o}C)	Heat of fusion (kJ/kg)	Thermal conductivity (W/m K)	Density(kg/m^3)
Palmitic acid	64	185.4	0.162 (liquid, 68.4 ^{o}C)	850 (liquid, 65°C) 989 (solid, 24°C)
Capric acid	32	152.7	0.153 (liquid, 38.5 ^{o}C)	878 (liquid, 45°C) 1004 (solid, 24°C)
Caprylic acid	16	148.5	0.149 (liquid, 38.6 ^{o}C)	901 (liquid, 30°C) 981 (solid, 13°C)
Propyl palmiate	16-19	186	n.a.	n.a.
Myristic acid	54	187	n.a.	0.844(80°C)
Lauric acid	42 - 44	178	0.147(50°C)	0.870(50°C)
Stearic acid	70	203	0.172(70°C)	0.941(40°C)

1.3 Literature Review

Hasan (1994) emphasized that myristic acid, palmitic acid and stearic acid are suitable materials for domestic water heating system. Thermophysical properties of those fatty acids have determined by using differential scanning calorimetry (DSC) and latent heat, specific heat and density, phase change temperature of those fatty acids was investigated. In addition, thermal cycling test was carried out to examine the stability of PCMs. As a result, the investigated fatty acids have suitable transition temperature for domestic water heating systems. The melting temperature of myristic acid, palmitic acid and stearic acid was found to be 50-54°C, 58-62°C and 65-69°C respectively. In addition, he has obtained that they have high latent heat values 189 kJ/kg for myristic acid, 201kJ/kg for palmitic acid and 210 kJ/kg for stearic acid.

Sari and Karaipekli (2012) prepared fatty acid esters-based composite PCMs for thermal energy storage. They observed that erythritol tetrapalmitate (ETP) and erythritol tetrastearate (ETS) are suitable candidates for thermal energy storage applications in buildings. They also added expanded graphite at different mass fraction (2%, 5%, and 10%) to increase thermal conductivity of the composite PCMs.

Properties of the prepared composite PCMs were determined by DSC. Moreover, they have carried out 1000 melting and freezing cycling to analyze thermal reliability and chemical stability. They observed that ETP and ETS are suitable candidates for thermal energy storage applications in buildings. After thermal cycles of PCMs, they have decided that PCMs have good thermal reliability and chemical stability.

Fauzi et al. (2013) identified myristic acid (MA) and palmitic acid (PA) as eutectic PCMs. They have prepared composite PCM with adding sodium myristate, sodium palmitate and sodium stearate into the MA/PA eutectic mixture. They evaluated thermal properties and thermal conductivity of eutectic PCM. They also observed that adding different range of surfactants increased the thermal conductivity of eutectic mixture. Moreover, the loading of surfactant indicated an important effect on reducing supercooling temperature. The latent heat of fusion also relatively increased by adding surfactants. As a result, it was observed that MA/PA eutectic mixture has a great potential to be applied as PCMs in thermal energy storage systems.

Sari (2003) combined two fatty acids, Myristic acid (MA) (58.0 wt. %) and Palmitic acid (PA) (42.0 wt. %), to generate a new kind of PCM which is suitable for moderate temperature applications, such as passive solar heating. MA-PA eutectic mixture has had 42.6°C melting temperature and 169.7 J/g. Thermal performance of this PCM is also evaluated in a concentric shell and tube type heat exchanger under various Stefan and flow Reynolds numbers. Comparative results indicate that the eutectic PCM melts and freezes at a constant temperature of 42.6°C, without any subcooling effect.

Wang et al. (2013) combined Lauric and Capric acid to obtain a eutectic PCM which is suitable for cold storage. In order to reduce the phase change temperature of the mixture, they have tried many additives in different molar fractions. As a result, they have suggested that the most appropriate combination for cold storage application is the addition of oleic acid with a mole fraction of 0.08 into the eutectic mixture. Heat of fusion and thermal conductivity of Capric-Lauric acid was found

115.1 kJ /kg, 0.572 Wm^{-1}K^{-1} respectively, with additives at mole fraction of 0.08 into the eutectic mixture.

Sari et al. (2009) prepared a form-stable composite PCM with adding Lauric acid (LA) into the Expanded Perlite (EP). They decided Lauric acid has a suitable melting and freezing point of 44.12°C and 40.97°C respectively. It also has latent heat of 93.36 J/g and 94.87 J/g, respectively. According to result of the thermal characterization analyses, the form-stable composite PCM has a good thermal reliability and chemical stability. Additionally, thermal conductivity of the form-stable LA-EP composite PCM is enhanced approximately 86% by incorporation of 10 wt. % expanded graphite.

Zhang et al. (2013) prepared eutectic PCM with combination of Lauric-Palmitic-Myristic acid. The mixture was then absorbed into the graphite. They have reported that the thermal conductivity of the composite PCM increases from 0.21 W/mK to 1.67 W/mK after the expanded graphite loading. The result of LA-PA-MA and LA-PA-MA/ EG show that the phase change temperature and latent heat of those PCMs were 31.41°C, 30.94°C and 145.8 J/g, 135.9 J/g, respectively.

Yang et al. (2014) synthesized Myristic-Palmitic-Stearic acid with expanded graphite. Results reveal that the optimum ratio of the expanded graphite in the eutectic mixture of Myristic-Palmitic-Stearic acids 13:1. Results also show that the integration of expanded graphite into the eutectic mixture raises the thermal conductivity from 0.25 W/mK to 2.51 W/mK. The melting and freezing temperatures and latend heats of the MA-PA-SA/EG composite PCM were 41.64°C and 42.99°C, and 153.5 J/g and 151.4 J/g respectively.

Sari et al. (2008) prepared fatty acid/expanded graphite (EG) composite PCMs. They have considered Capric acid (CA), Lauric acid (LA) and Myristic acid (MA) as pure PCMs in the preparation of composites. In addition to the DSC and SEM analyses, they have also carried out an experimental work within a constant temperature bath to compare the melting and solidification durations of pure and

composite PCMs. Result show that the phase change temperature of composite PCMs remain almost constant comparing to the pure PCMs, but the latent heat of fusion values decrease more than 20% for all cases. It is also reported that, solidification durations of CA/EG, LA/EG and MA/EG composite PCMs were reduced by 68%, 33% and 56% respectively, comparing the pure ones. Similarly, in terms of the melting durations, reductions of 17%, 22% and 53% were observed for CA/EG, LA/EG and MA/EG composite PCMs, respectively.

Mehrali et al. (2013) investigated palmitic acid/graphene nanoplatelets (PA/GNPs) as a composite PCM. They have prepared a shape stable composite PCM, which means that PA was absorbed by GNPs so that there is no leakage of PA at the end of discharging period. Results indicate that the thermal conductivity value of the PA/GNPs composite with 77.99% (wt.) of PA is 10 times higher than pure PA. Experimental finding also reveal that, while the pure PA needs 360 s to reach the phase change temperature, the time is needed for the PA/GNPs composite with 77.99% (wt.) PA is only 150 s.

Wei et al. (2014) prepared Capric acid/expanded perlite (CA/EP) and Capric-stearic acid/expanded perlite (CA-SA/EP). They have measured latent heat values of CA/EP composites are 87.3 J/g and 89.0 J/g for the melting and freezing process, respectively. CA-SA/EP has latent heat of 82.1 J/g and 82.6 J/g. Moreover, thermal cycling test results show that the composites have good thermal reliability and good chemical stability.

1.4 Objectives

The main objective of the study is to increase thermal conductivity of Myristic acid (MA) and Arachidic acid (AA), without any change in the major properties such as heat of fusion and phase change temperature of Myristic acid and Arachidic acid, by adding GNP at different ratios (0.5%, 1% and 2%). For this purpose, Myristic acid/Graphite nanoplates (MA/GNP) and Arachidic acid/Graphite nanoplates

(AA/GNP) composites were prepared and evaluated in terms of thermal conductivity, melting/freezing temperatures, and latent heat values of melting and freezing.

According to the recent research of the authors, AA has never been used as a PCM in the literature. In order to investigate the thermal characteristics of the AA and MA/GNP, AA/GNP composites, several thermal analyses are conducted such as; scanning electron microscopy (SEM), thermogravimetric analysis (TGA), differential scanning calorimetry (DSC), fourier transform infrared (FTIR), X-ray diffraction analysis (XRD) and thermal conductivity measurements. In addition, GNP is incorporated into the AA and MA with various fractions, to compose new composite PCMs with higher thermal conductivity values. Moreover, the chemical and thermal stabilities of MA/GNP and AA/GNP composite PCMs were investigated at various thermal cycles (1, 10, 40, 70 and 100 cycles).

CHAPTER TWO
MATERIALS AND METHODS

2.1 Materials

In this study, Myristic acid (MA) (chemical formula: $C_{14}H_{28}O_2$, formula weight: 228 g/mol) and Arachidic acid (AA) (chemical formula: $C_{20}H_{40}O_2$, formula weight: 312.54 g/mol) were used as PCM in the preparation of the composite PCMs. These materials were supplied from Alfa Aesar and used without further purification. According to the catalogue of the producer, phase change temperature of MA and AA are in the range of 50 °C to 60 °C, 74 °C to 76 °C, respectively. Graphite nanoplates (GNP) were used to improve the thermal properties of the MA and AA. In the current study, GNP was obtained from *Graphite Chemical Industries Company* (Ankara, Turkey). The particle size, thickness and surface area of the GNP are 5 μm, 5-8 nm and 120-150 m^2/g, respectively.

2.2 Synthesis

2.2.1 Preparation of Myristic Acid/Graphite Nanoplates and Arachidic Acid/Graphite Nanoplates Composites PCMs

For Myristic acid (MA); as a first step, Myristic acid is heated to a temperature of 60°C in an incubator to ensure that MA is in the liquid phase. Then, GNP loading is performed in the liquid phase at different rates. After these operations, mixing process is carried out using an ultrasonic homoginazator (Misonix, Sonicator 3000) for approximately two minutes to procure homogeneous distribution. In the composite, different rate of the GNP as 0.5%, 1% and 2% were added in order to determine the effect of GNP additive on the thermal conductivity of MA.

For Arachidic acid (AA); it was first converted into the liquid phase by heating at 76 °C and then different amounts of GNP (0.5%, 1% and 2%) were incorporated into the molten material. In order to achieve better dispersion of GNP into the Arachidic

acid, the mixture was mixed thoroughly with an ultrasonic homogenizer (Misonix, Sonicator 3000) for two minutes. Eventually, the mixture was cast into a petri dish and dried in an oven at 60 °C.

2.3 Instrumentation

2.3.1 Differential Scanning Calorimetry (DSC) Analysis

Melting and freezing temperatures, latent heat values of melting and freezing of PCMs were determined differential scanning calorimeter (DSC; Perkin Elmer-Diamond). DSC was used for thermal properties of the PCMs. The mass of the samples in the current work varied between 2 and 10 mg. Samples were encapsulated in an aluminum pan and sealed. The samples were scanned with heating and cooling rate of 1°C/min over the range from 45 to 65°C for MA, from 65 to 85°C for AA under nitrogen atmosphere. Specifications for the device are given Table 2.1 (Erek and Ezan, 2011).

Table 2.1 Technical features of the DSC equipment (Erek and Ezan, 2011)

Brand, model		Perkin Elmer, Diamond DSC
Temperature	Operating range	170°C-730 °C
	Accuracy	±0.1°C
	Resolution	±0.01°C
Calorimeter	Accuracy	<±1%
	Resolution Precision	<±0.1%
	Dynamic range	0.2 µW
		0.2 µW-800mW
Scan speed	Heating	0.01°C/min 500°C/min
	Cooling	0.01°C/min 500°C/min

There are two micro ovens in which the sample and reference materials are settled inside the DSC. In Figure 2.1, schematic representation regarding the oven and photographs are given to existing systems.
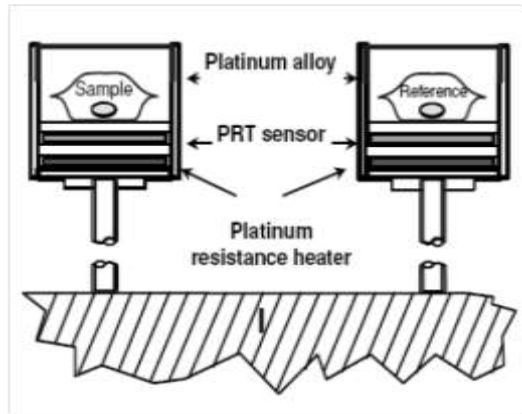
(a) Schematic representation   **(b)** Existing system

Figure 2.1 Sample and reference ovens for DSC (Erek and Ezan, 2011)

Empty sample containers are widely used in applications as reference material. Because, in this case the obtained DSC curves reflects only heat exchange in the sample container. In DSC measurements, obtained endothermic or exothermic peaks are analyzed by making adjustments with curve of the empty containers. The curve of empty containers expresses while sample containers completely empty performed analysis. Structural differences between the sample and reference ovens and thermal behaviour of the sample containers are removed from the test results by using curve of the empty containers. Sample containers are fixed-volume containers that made of aluminium and stainless steel in DSC. Containers can be used as indoor or outdoor depending on the properties of the examined sample (Erek and Ezan, 2011).

For the heat flow calibration of the device, indium and zinc reference were used and the temperature calibration was carried out by indium and zinc references. Moreover, the heat and temperature calibration of the device was performed by using sapphire as an internal reference. Calibration was carried out consistently prior to the first analyses of each weekday (Erek and Ezan, 2011).

Thanks to DSC, latent heat of melting and freezing, melting and freezing temperatures, solid and liquid phase specific heat values, the changes in thermal performance after certain number of thermal cycling processes were obtained.

2.3.2 Thermogravimetric Analysis (TGA)

Thermogravimetric analysis was carried out by using Perkin-Elmer Diamond TG/DTA analyzer. The analyses were performed at a heating rate of 10 °C/min over the range from 30°C to 600°C, under inert nitrogen atmosphere. Thermogravimetric analysis was used for the determination of thermogravimetric decomposition of the composites as a function of the temperature.

The reference weight with known standard mass was used for the weight calibration and the temperature calibration was carried out by starting the automatic sensor calibration of the device. Calibration was actualized systematically prior to the first analyses of each weekday.

Decomposition behavior and thermal stabilities of pure AA, MA and composite PCMs (AA/0.5%GNP, AA/1%GNP, AA/2%GNP and MA/0.5%GNP, MA/1%GNP, MA/2%GNP) were determined thanks to Perkin-Elmer Diamond TG/DTA analyzer.

2.3.3 Fourier Transform Infrared Spectroscopy (FTIR) Analysis

Fourier transform infrared spectroscopy (FTIR) analysis was carried out by using Perkin Elmer Spectrum BX-II FTIR spectrometer. After drying and grinding process of composite PCMs, 1 mg of samples was mixed with approximately 100 mg of high purity infrared-grade KBr. Then the mixture was compressed into pellets. FT-IR spectra of composite PCMs were recorded in between 4000-400 cm^{-1} with a resolution of 2 cm^{-1} and 25 scans.

2.3.4 Scanning Electron Microscope (SEM) Imaging

The surface morphologies of composite PCMs were investigated by a FEI Quanta FEG 250 scanning electron microscope (SEM) at an accelerating voltage of 2 kV in the secondary electron mode.

2.3.5 Thermal Conductivity Measurements

In the current study, 3ω thermal conductivity measurement was applied to achieve the thermal conductivity of PCMs. These measurements were carried out while PCMs are molten. Thermal conductivity measurements of the PCMs for the liquid phase were carried out by a technique based on a hot wire thermal probe with AC excitation and 3ω lock-in detection. This method is called 3ω method. A thin metal wire submerged into a liquid sample acts as a heater and thermometer. Ni wire with dimensions of 40 μm in diameter and $2l = 19.0$ mm long is used as a thermal probe (ThP). An alternating input current with frequency of ω heats the wire consequently the sample with 2ω frequency. Since electrical conductivity of metal varies linearly with temperature, output voltage includes 3ω component which depends on thermal conductivity of the sample. The method was validated with pure fluids, such as water, methanol, ethanol and ethylene glycol and yielding accurate thermal conductivity ratios within $\pm 2\%$. Installation of thermal conductivity measurement method of 3ω is shown in Figure 2.2. The details of the setup can be obtained elsewhere (Tavman & Turgut, 2010; Turgut et al., 2008).
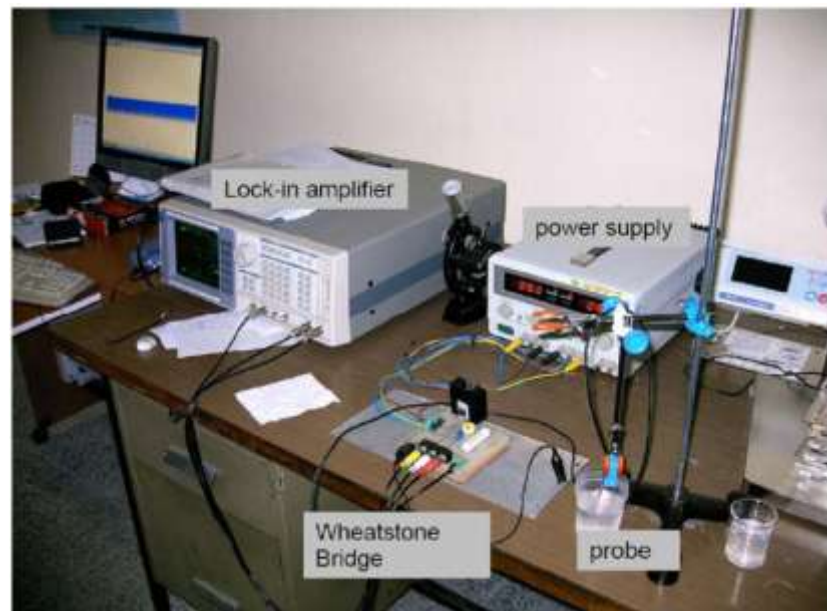

Figure 2.2 The main components of the thermal conductivity measurement device

2.3.6 Thermal Cycling Test

Thermal reliability of composite PCMs was investigated by the thermal cycling tests. The variation in latent heat values and phase change temperatures were determined as a function of thermal cycling number. At the end of 10, 40, 70 and 100 thermal cycles, the chemical and thermal stabilities of composite PCMs were shown by DSC and FT-IR analyses. DSC analyses were performed with 5°C/min of constant scan rate and for a temperature range between 45°C and 65°C, 65°C and 85°C for thermal reliability of MA/GNP and AA/GNP composite PCMs, respectively under a constant stream of nitrogen.

CHAPTER THREE
RESULTS AND DISCUSSION

3.1 SEM Analysis of AA/GNP and MA/GNP Composite PCMs

Representative SEM images of the AA and the composites of AA/0.5%GNP, AA/1%GNP and AA/2%GNP were presented in Figures 3.1-3.4. A smooth surface can be seen in SEM image of AA, as pictured in Figure 3.1. After GNP loading, slightly modifications occur in the surface of the AA. As can be seen from Figure 3.2, 3.3 and 3.4 GNP tends to from agglomerates. When amount of GNP is increased in AA, enlargement of agglomerates is seen clearly. This is equivalent to stating that the greatest formation of agglomerates can be noticed in the 2%/GNP concentration in this study. It is seen on Figure 3.4.
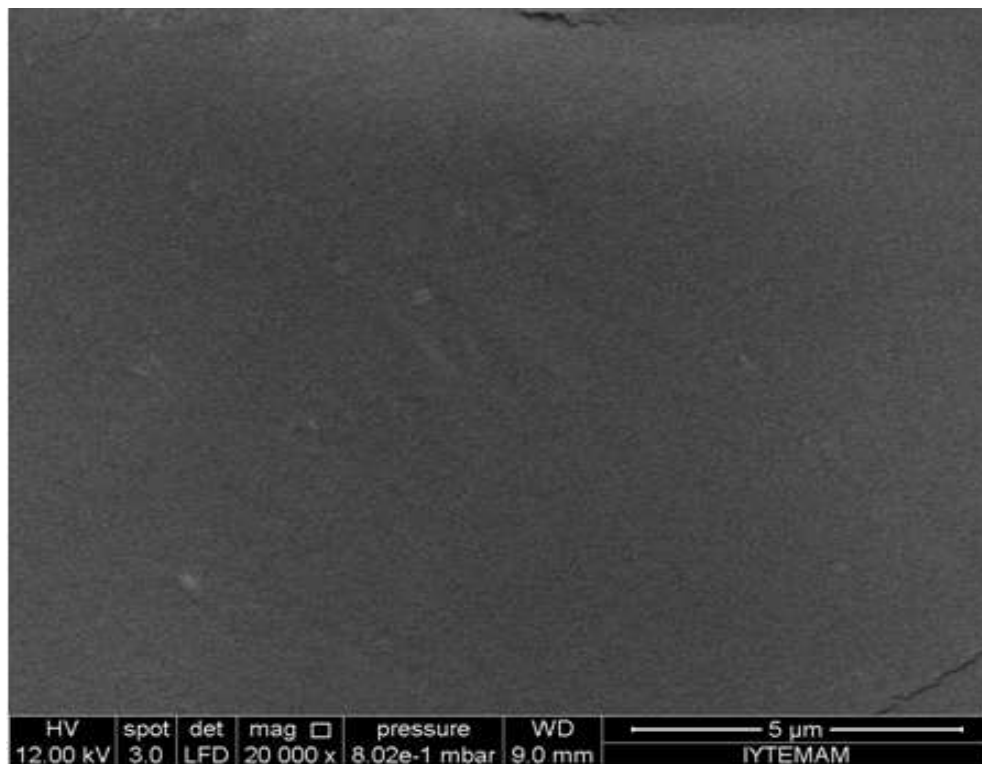

Figure 3.1 SEM micrographs of AA

Figure 3.2 SEM micrographs of AA/0.5%GNP composite PCM
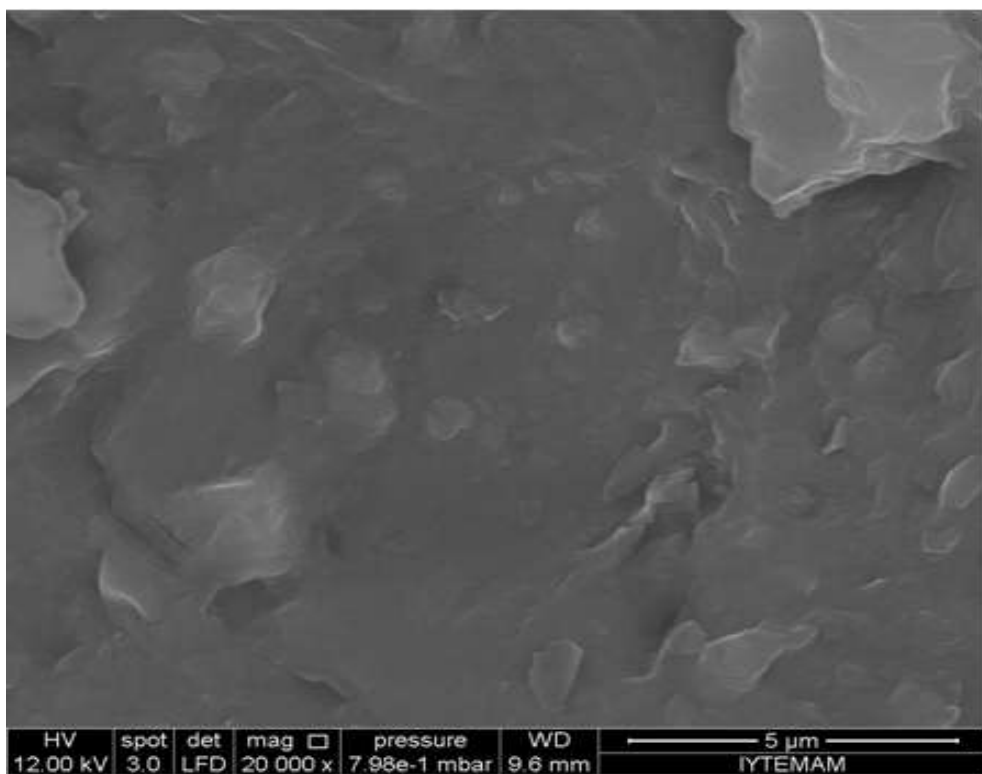
Figure 3.3 SEM micrographs of AA/1%GNP composite PCM

Figure 3.4 SEM micrographs of AA/2%GNP composite PCM

Figures 3.5 to 3.8 present the SEM images of MA and MA/0.5%/GNP, MA/1%GNP and MA/2%GNP, respectively. It can be seen from Figure 3.5 that pure MA has a foliaged structure. After the addition of GNP, the surface of MA changes considerably. As the GNP loading increased to 2 wt. %, as shown in Figure 3.8, the GNP particles are connected with each other to form a compact striped that surround the MA particles. The GNP is observed successfully in the pores structure of the pure MA.
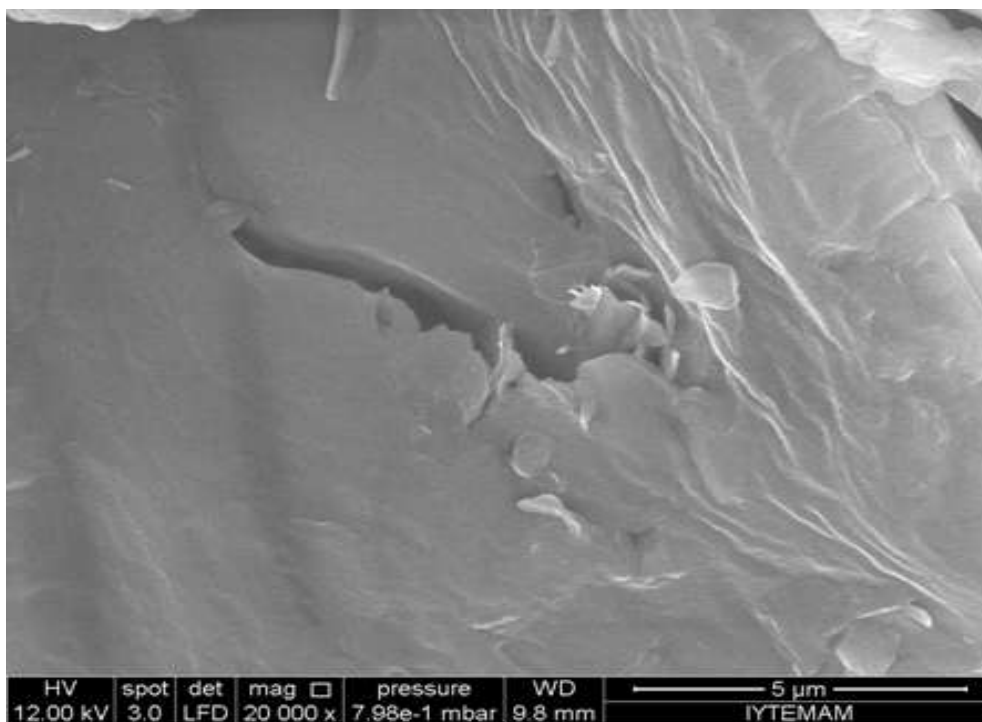
Figure 3.5 SEM micrographs of MA

Figure 3.6 SEM micrographs of MA/0.5%GNP composite PCM
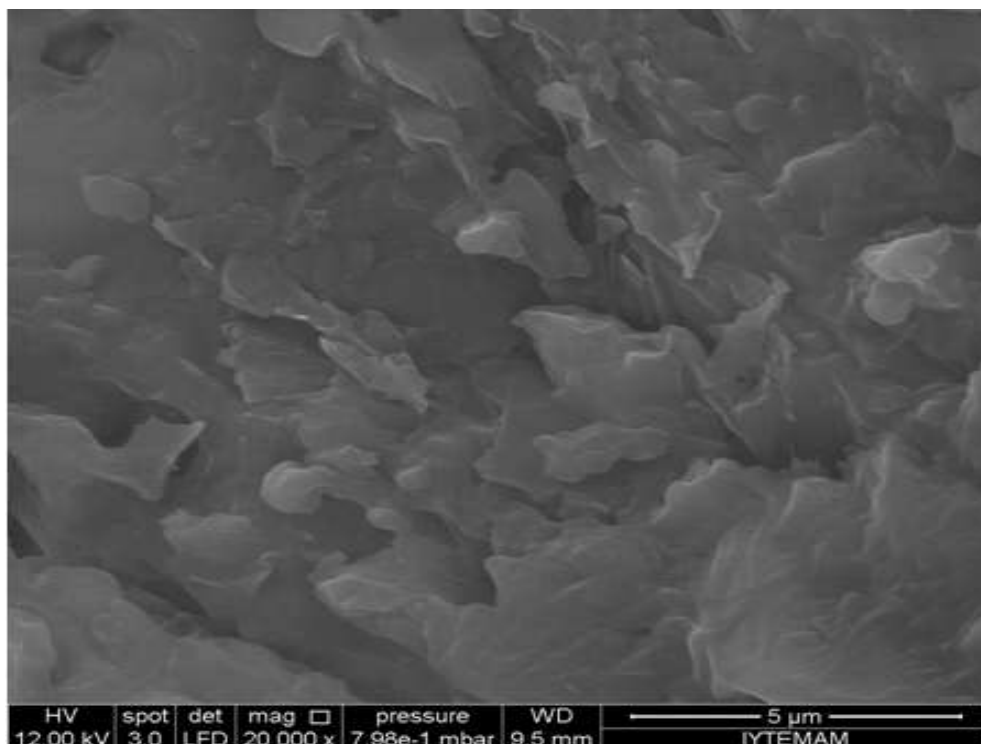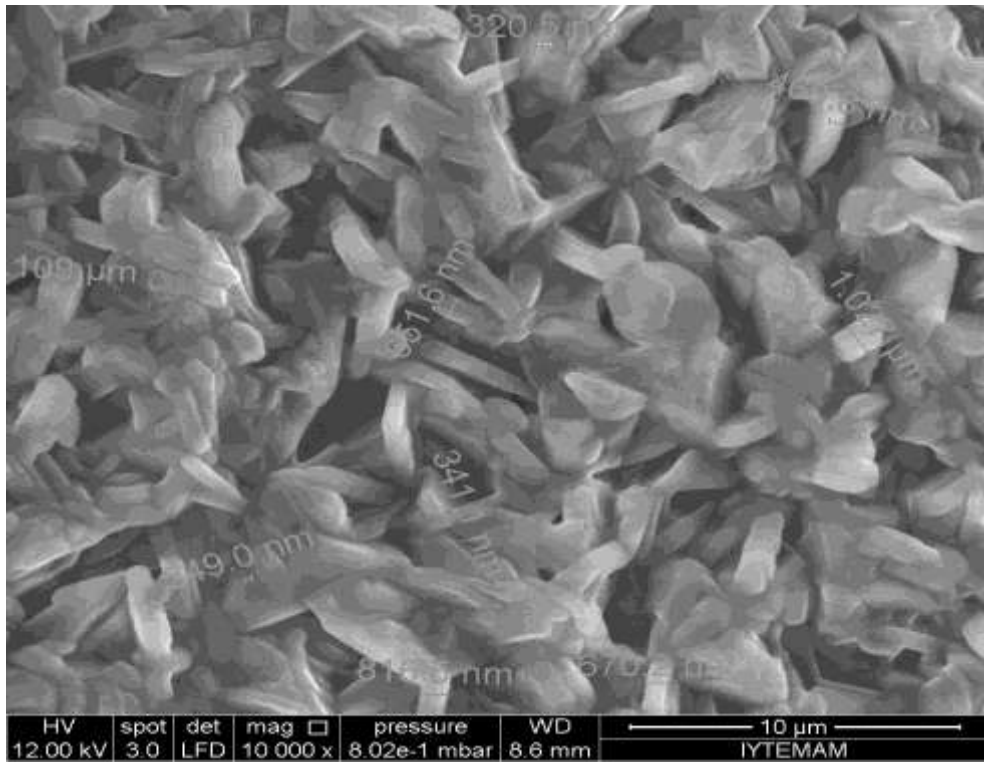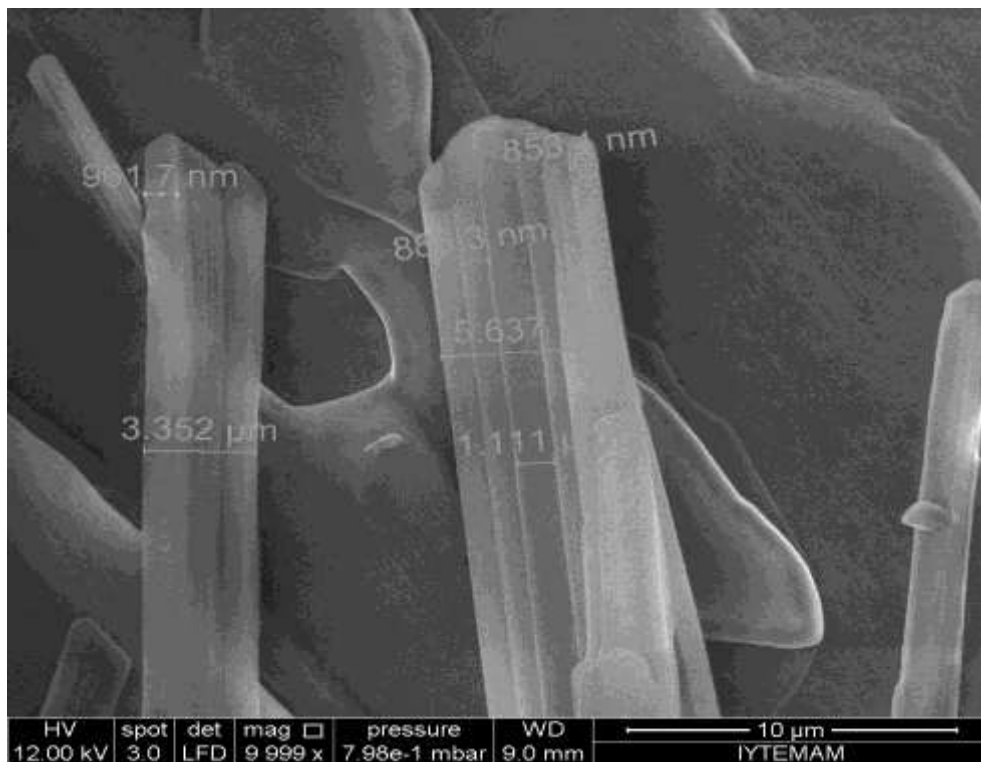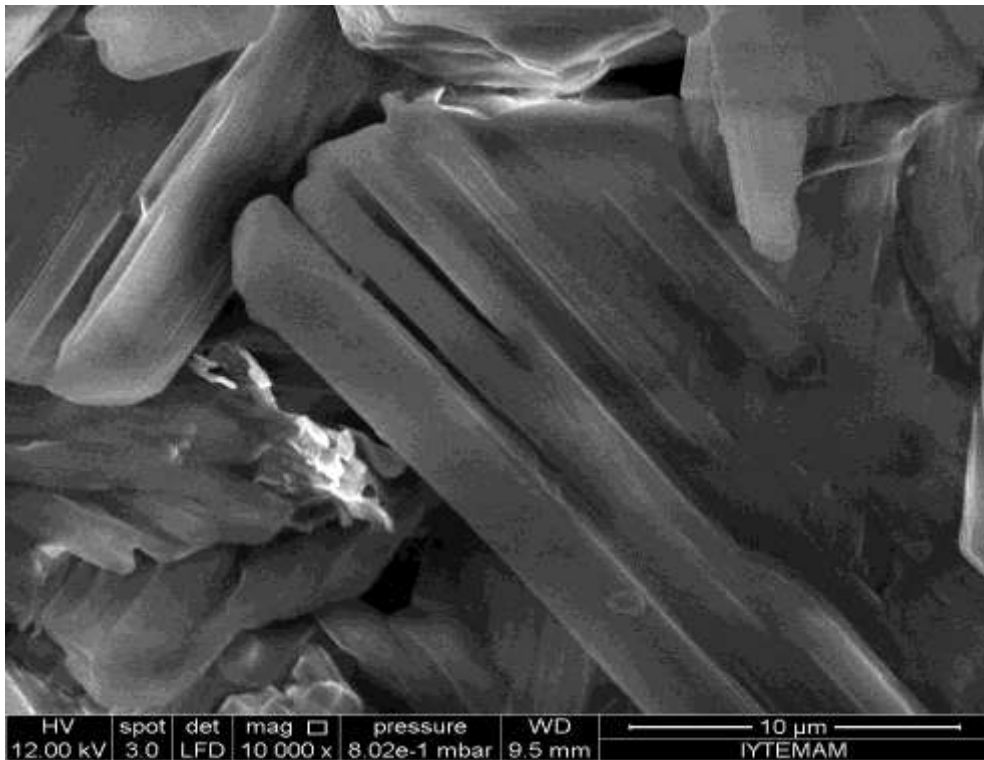
Figure 3.7 SEM micrographs of MA/1%GNP composite PCM
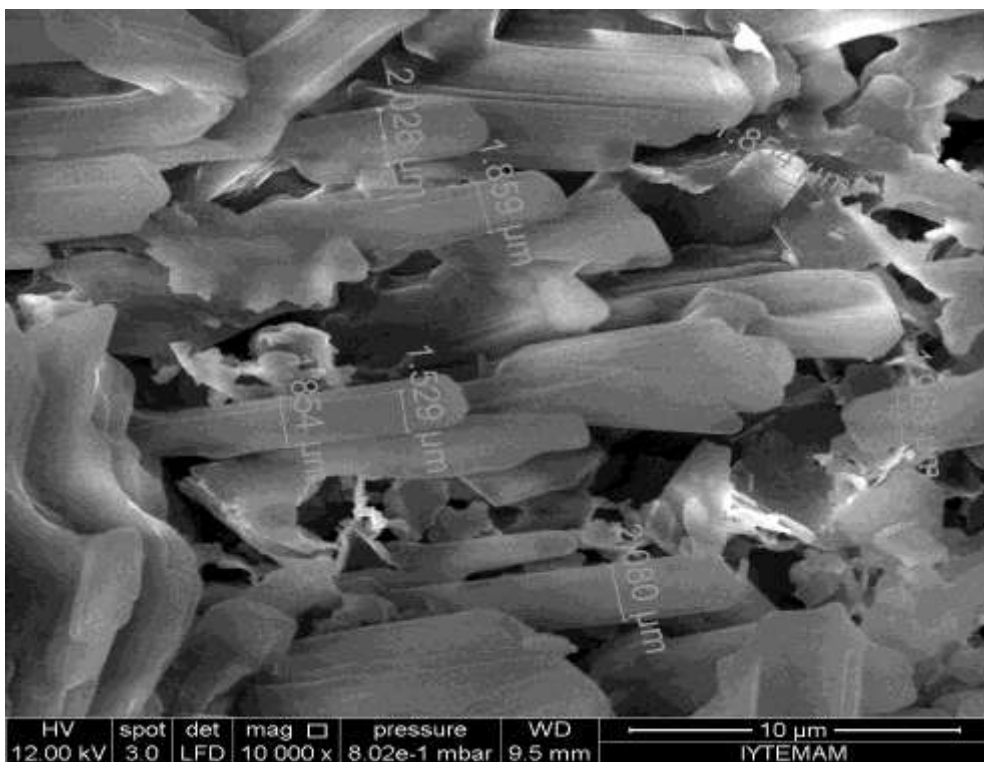
Figure 3.8 SEM micrographs of MA/2%GNP composite PCM

3.2 FTIR Analysis of AA/GNP and MA/GNP Composite PCMs

Figure 3.9 shows FTIR spectra of AA, AA/0.5%GNP, AA/1%GNP and AA/2%GNP. The band at $1700 cm^{-1}$ is based on C=O group of AA. After 1% of GNP loading, this band is seen at $1709 cm^{-1}$. However, GNP loading of 2% into the AA did not cause variation. The asymmetrical vibrations of CH_2 were ascertained at 2919 and $2850 cm^{-1}$, respectively. No significant variation in these bands was realized after GNP loading. However, absorption band of CH_2 groups at $1428 cm^{-1}$ cannot be seen for 2% GNP loading in AA. As can be seen from Figure 3.9, in-plane and out-plane bending vibrations of the –OH groups exhibit the absorption bands at $1460 cm^{-1}$, 1298 and $945 cm^{-1}$, $682 cm^{-1}$, respectively. The band corresponding to $682 cm^{-1}$ (out-of-plane bending) was not observed in the spectrum of AA/2%GNP (Sari et al. 2013). The C-O stretching vibrations in carboxylic acid groups are noticeable around $1200 cm^{-1}$. The existence of GNP with an amount of 2 wt. % in AA inhibits the appearance of some bonds in AA. From FTIR spectra it is seen that no remarkable interaction takes place between GNP and AA.

Figure 3.9 FTIR the effect of GNP loading of AA on functional group

The effect of GNP loading on functional groups of MA was shown in Figure 3.10. The band corresponding to C=O stretching vibration of MA was observed at 1700 cm^{-1}, as presented in FTIR spectrum of MA. After GNP loading this band did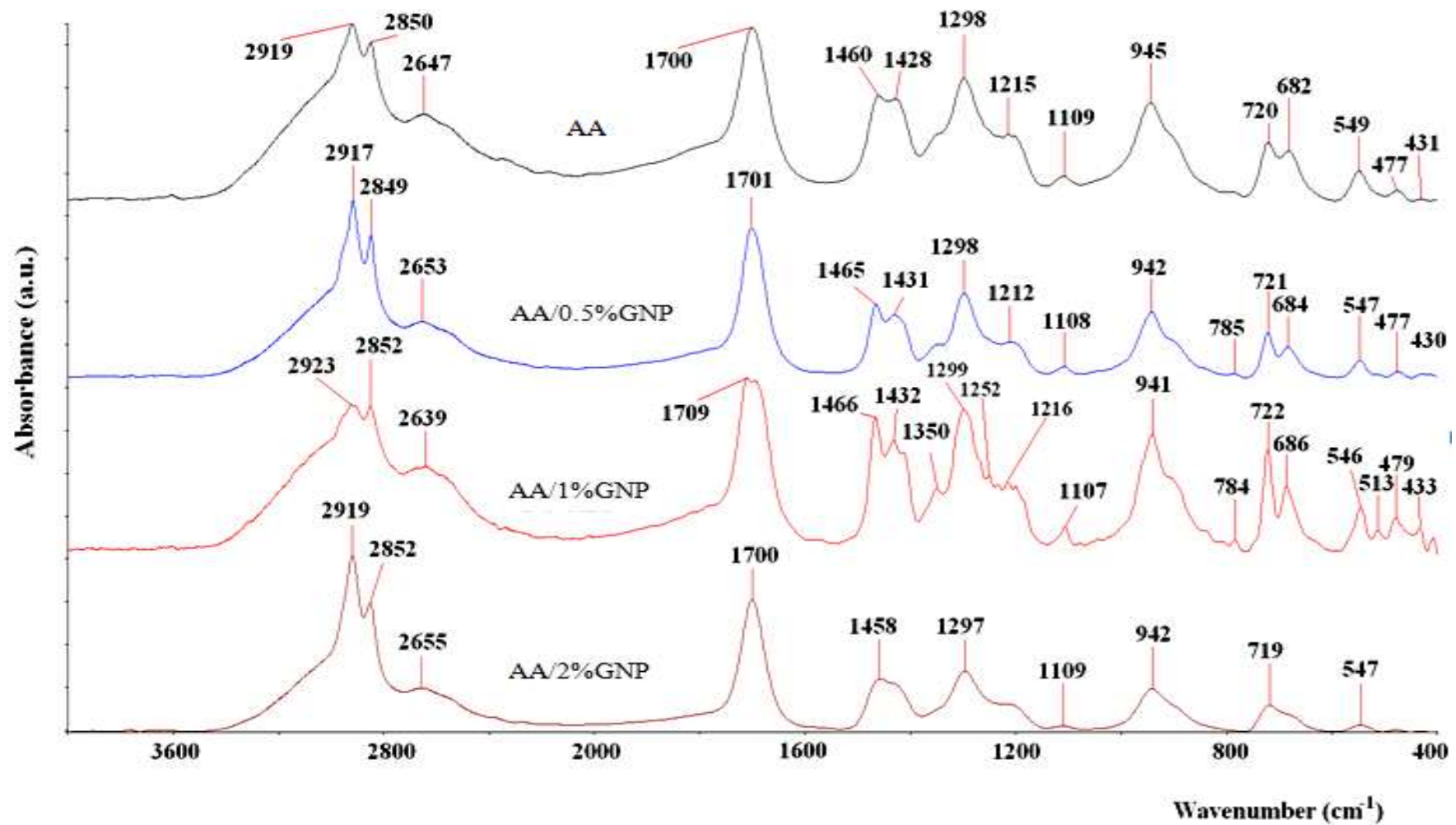 not change considerably. The absorption bands at 2916 and 2848 cm^{-1} show the asymmetrical and symmetrical vibration of functional group of $-CH_2$ (Karaipekli & Sari, 2008). The considerable changing appeared after the loading of MA with GNP of 2 wt. %. The bands at 1466 cm^{-1} and 1291 cm^{-1} (due to in-plane bending vibration of the –OH groups), 939 cm^{-1} and 685 cm^{-1} (out-of-plane bending vibration of the –OH group) is attractive. After the loading of MA with GNP of 2 wt. %, the band at 685 cm^{-1} cannot be directly seen. -OH swinging mode was observed at 723 cm^{-1} (Ferreira et al., 2002; Fang et al., 2010). The band at 1431 cm^{-1} in the spectrum of MA may be due to CH_2 groups in MA (Sari et al., 2013b). The C-O stretching vibrations in carboxylic acid groups are recognizable around 1200 cm^{-1}. Except for MA/2%GNP, these small bands can be seen for all composites. As can be seen from the spectrum of MA/2%GNP, greater amounts of GNP in MA/2%GNP composite may have showed the appearance of some bands in MA. There is no significant shift in the absorption bands of MA/GNP composite samples in comparison with that of MA, which shows that relatively weak chemical interactions between GNP and MA come into existence. Presumably, MA was held by capillary and surface tension forces within the pores of GNP. Thus, leaking of melted MA from MA/GNP composites may be inhibited.
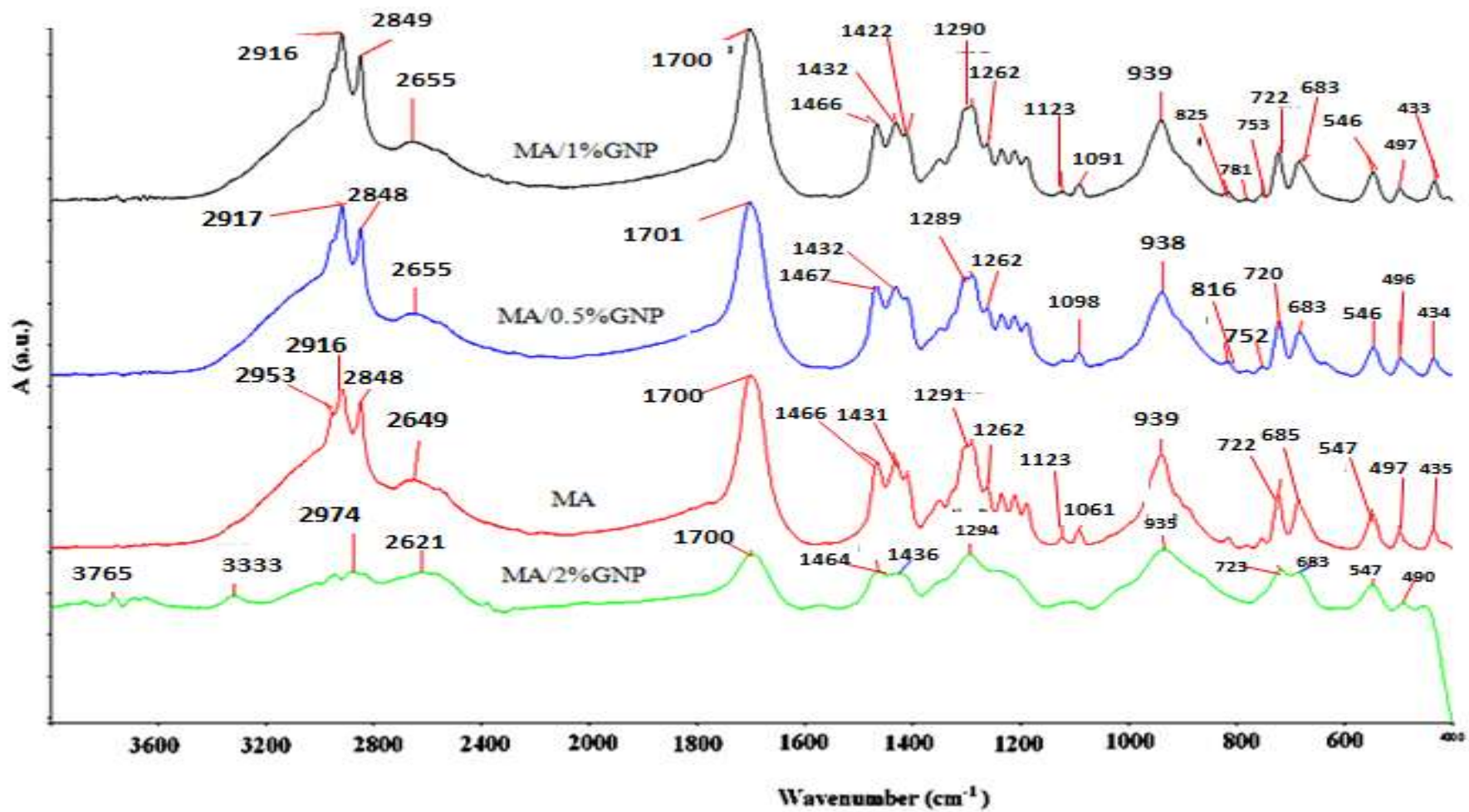
Figure 3.10 FTIR the effect of GNP loading of MA on functional group of MA

3.3 Thermal Properties of AA/GNP and MA/GNP Composite PCMs

Thermal properties of PCMs such as melting and freezing temperatures and latent heat values are the most significant parameters for a latent heat thermal energy storage system (Kousksou et al., 2014; Dincer & Rosen, 2002). The crystallinity fraction (*Fc*) of MA and AA in the composites was obtained by using following equation (Wang et al., 2012);

$$F_c = \frac{\Delta H_{composite}}{\Delta H_{pure} x \beta} 100\% \tag{3.1}$$

where ΔH_{pure} and $\Delta H_{composite}$ show the latent heat of pure AA or MA and the composites, respectively, and β indicates the amount of AA or MA in the composites.

DSC curves of AA/GNP composites were shown in Figure 3.11 and the obtained values were given Table 3.1. The crystallinity of AA composite decreased to 95.7% after 2 % GNP loading. It may arise from the fact that AA is partly embedded in the pores of GNP, the movement of the AA during the crystallization is restricted (Li et al., 2013). However, loading of 0.5% GNP did not cause any variation in terms of crystallinity of AA. Besides, as shown in Table 3.1, the degree of supercooling decreased from 1.5 to 0.3°C after 0.5% GNP loading of AA. 1% GNP loading of AA decreased the crystallinity of AA, but increased the extent of supercooling to 1.9°C. GNP loading of AA did not cause any variation in melting and freezing temperatures of AA, but slight decrements in melting and freezing latent heats. After 1% GNP loading of AA, melting temperature and latent heat of melting decreased from 75.2 to 74.8°C and 208 to 202 J/g, respectively. Freezing temperature did not change but freezing latent heat changed from -198 to -190 J/g.

Figure 3.11 DSC curves for AA/GNP composites

Table 3.1 DSC data for AA/GNP composite PCMs

Sample	Melting temperature	Melting Latent heat	Freezing temperature	Freezing Latent heat	Crystallinity of AA	Extent of supercooling
	T_m (°C)	ΔH_m (J/g)	T_f (°C)	ΔH_f (J/g)	F_c (%)	$T_m - T_f$ (°C)
AA	74.8	208	73.3	-198	100	1.5
AA/0.5%GNP	74.5	207	74.2	-191	100	0.3
AA/1%GNP	75.2	202	73.3	-190	98.1	1.9
AA/2%GNP	74.7	195	74.3	-184	95.7	0.4

Figure 3.12 shows DSC curves of MA/GNP composite PCMs and the results were summarized in Table 3.2. Composite, MA/GNP, formation did not affect the crystallinity fraction of MA at 2 wt. %. It may be due to the fact that MA was held within the pores of GNP, the movement of the MA during the crystallization process

was restricted. As can be seen from Table 3.2, the extent of supercooling was obtained to be 2.5°C for MA. However after loading of MA with GNP of 0.5%, the extent of supercooling decreased to 0.7°C. 2%/GNP loading led to the same result. It can be said that after composite formation, the extent of supercooling of MA was improved significantly at 0.5%/GNP loading. GNP loading of MA decreased the melting temperature of MA, by 0.7°C for GNP of 2%, but increased the freezing temperature of MA, by 1.1°C for GNP of 2%. The freezing latent heat of MA decreased from -177 J/g to -169 J/g with the treatment of GNP of 2%. However GNP loading of MA did not almost vary the melting latent heat of MA.
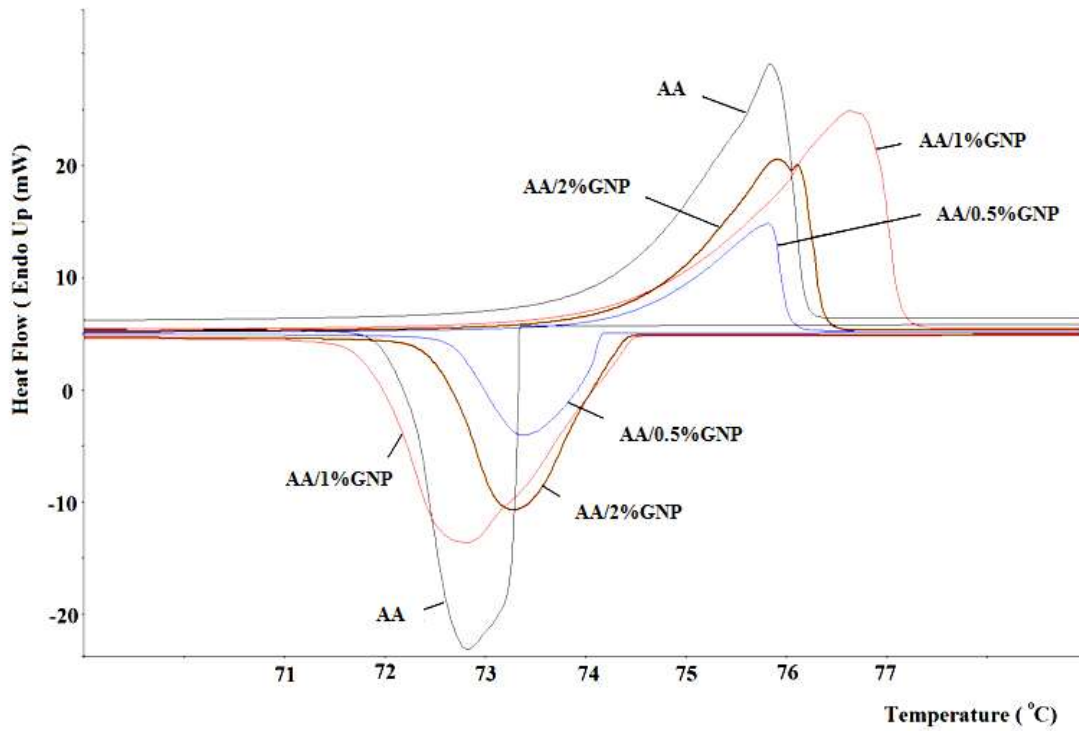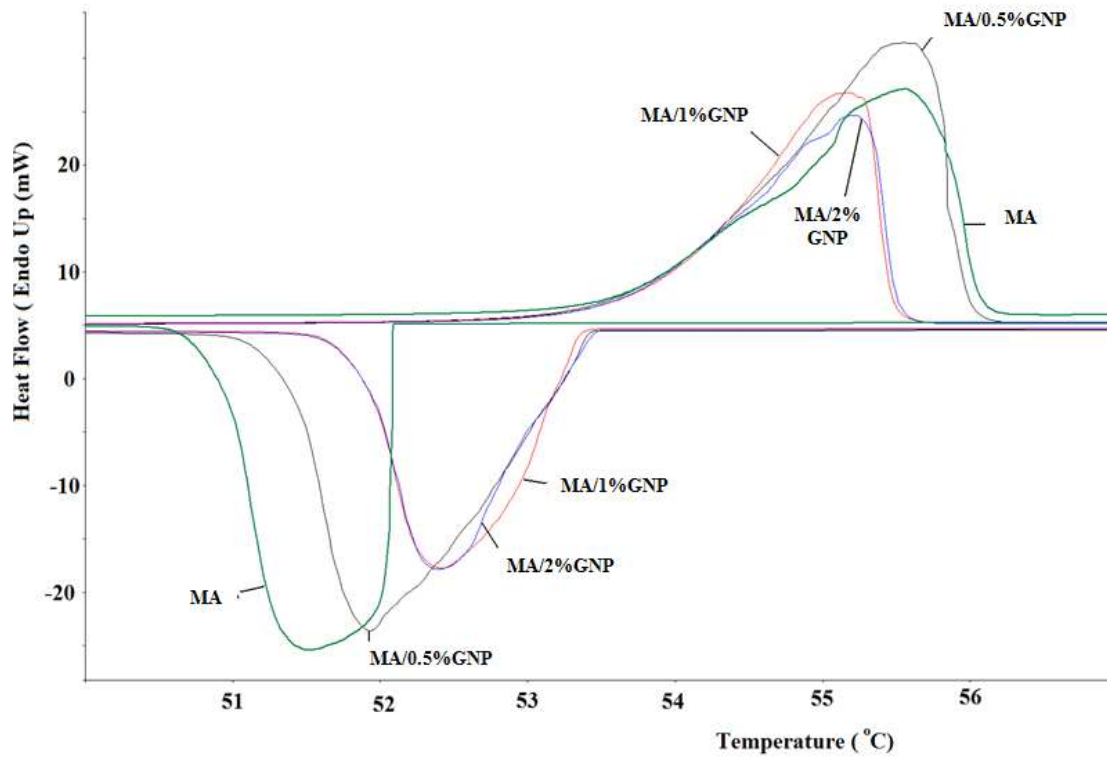

Figure 3.12 DSC curves for MA/GNP composites

Table 3.2 DSC data for MA/GNP composite PCMs

Sample	Melting temperature	Melting Latent heat	Freezing temperature	Freezing Latent heat	Crystallinity of MA	Extent of supercooling
	T_m (°C)	ΔH_m (J/g)	T_f (°C)	ΔH_f (J/g)	F_c (%)	$T_m - T_f$ (°C)
MA	54.6	181	52.1	-177	100	2.5
MA/0.5% GNP	54.1	181	53.4	-175	100	0.7
MA/1% GNP	54.0	181	53.3	-174	100	0.7
MA/2% GNP	53.9	177	53.2	-169	100	0.7

3.4 Thermal Stability of Composite PCMs

The thermal stabilities of the composite PCMs were evaluated by TGA. TGA curves of AA and AA/GNP composites are presented in Figures 3.13 to3.16. Figures 3.13 to 3.16 show that pure AA and all of composite PCMs are degraded in a single step. Pure AA protected its stability up to 178°C and then as the temperature reaches to 302°C, 89.2% weight loss was observed. AA/0.5%GNP, AA/1%GNP and AA/2%GNP protected their stability up to 180°C, 173°C and 178°C, respectively. When composite PCMs exceed these temperatures, decomposition began in the materials. Weight loss of these materials was obtained as to 79.1%, 91.1% and 90.8 %, respectively. Finally, GNP addition does not cause any major change on the degradation mechanisms. TGA data for AA and AA/GNP composite PCMs were given in Table 3.3.
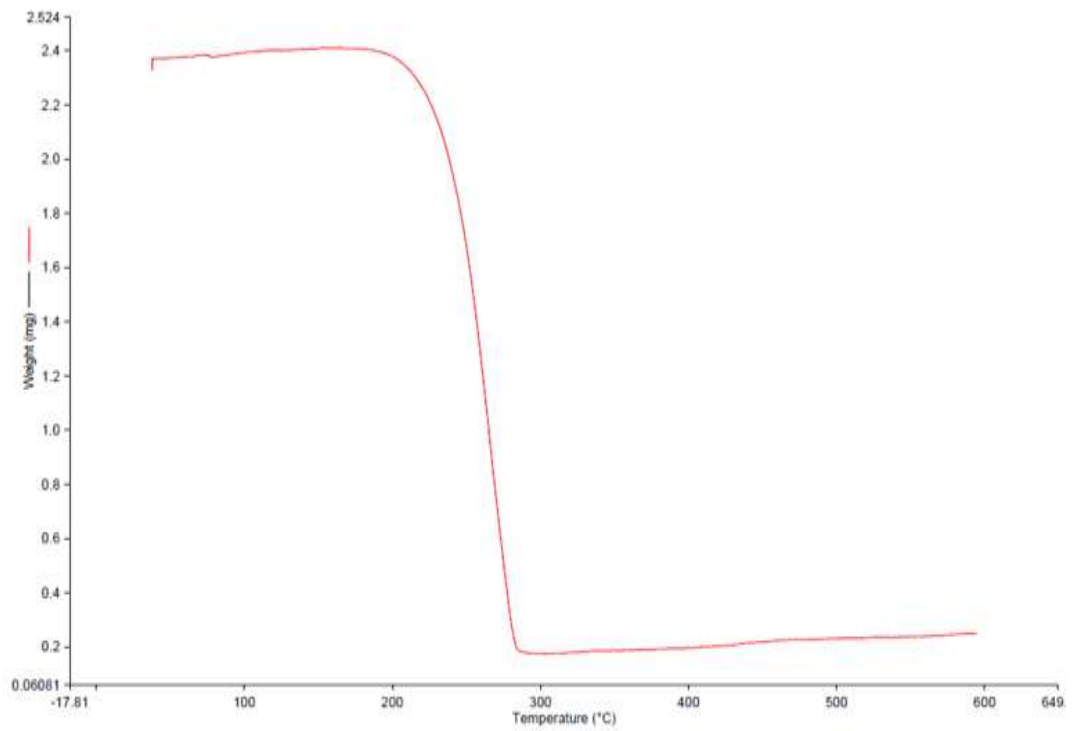
Figure 3.13 TGA curves of pure AA

Figure 3.14 TGA curves of AA/0.5%GNP composite PCMs

36

Figure 3.15 TGA curves of AA/1%GNP composite PCMs

Figure 3.16 TGA curves of AA/2%GNP composite PCMs

TGA curves of MA and MA/GNP composite PCMs were presented Figures 3.17 to 3.20. Figures 3.17 to 3.20 show that pure MA and all of composite PCMs are decomposed in a single step. Pure MA protected its stability up to 131°C and then when it was reached at 260°C, has 95.1% weight loss. MA/0.5%GNP, MA/1%GNP and MA/2%GNP protected their stability up to 125°C, 128°C and 131°C, respectively. When composite PCMs exceed these temperatures, decomposition began in the materials. Weight loss of these materials was obtained as to 90%, 96.7% and 95.0% respectively. Finally, GNP addition does not cause any major change on the degradation mechanisms. In Table 3.4, TGA data of pure MA and MA/GNP composite PCMs were given.
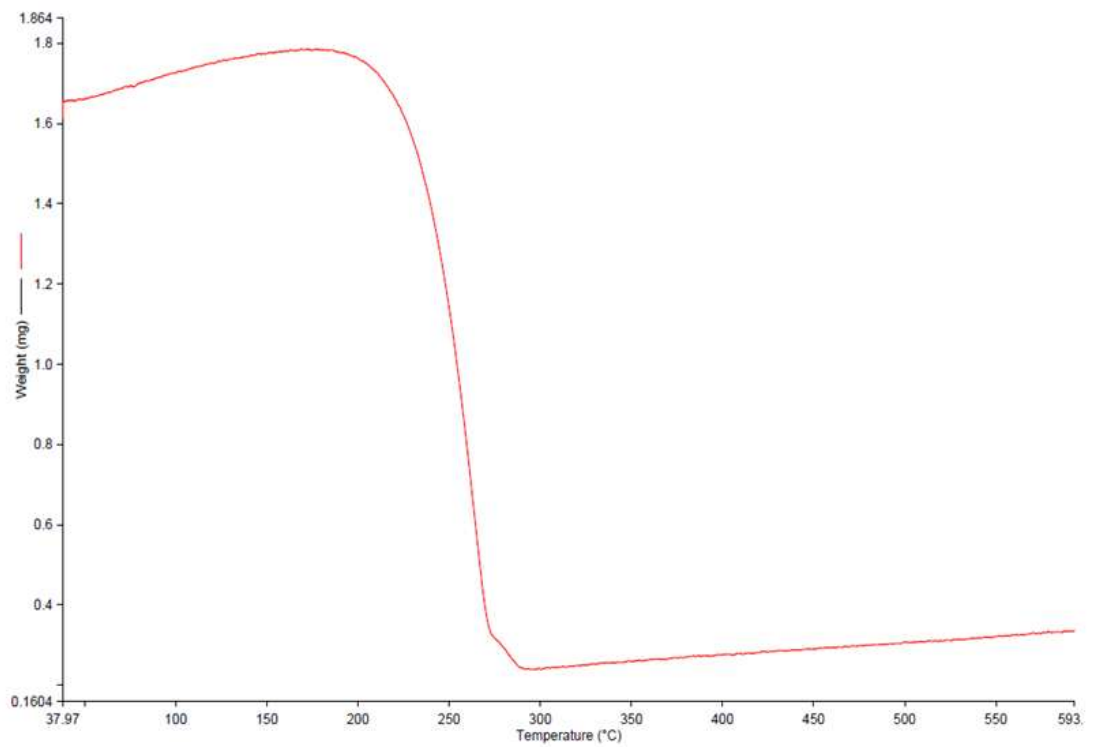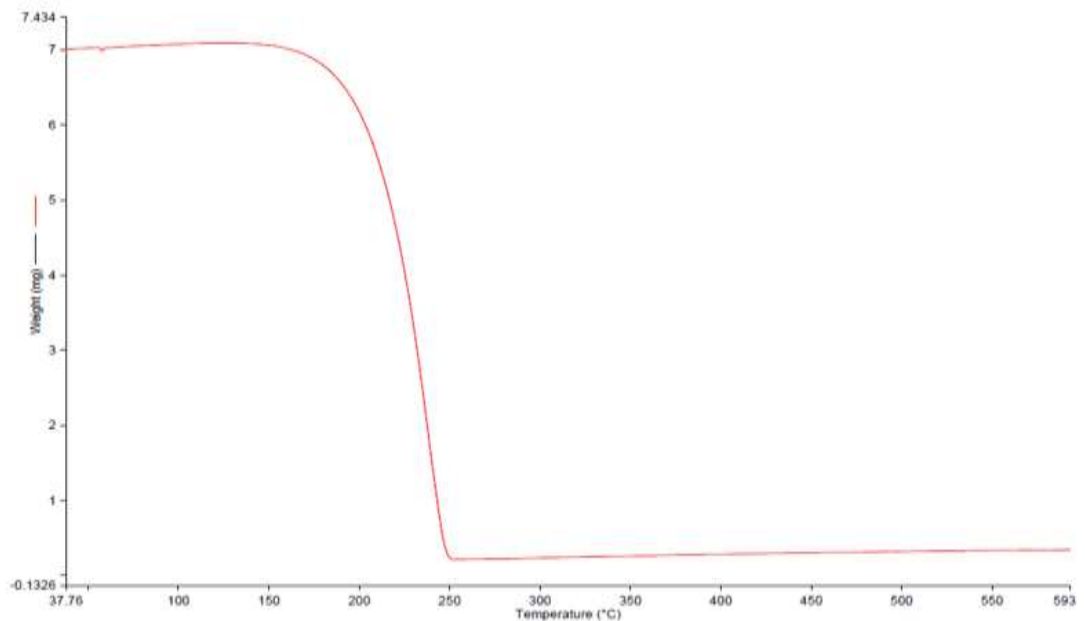

Figure 3.17 TGA curves of pure MA
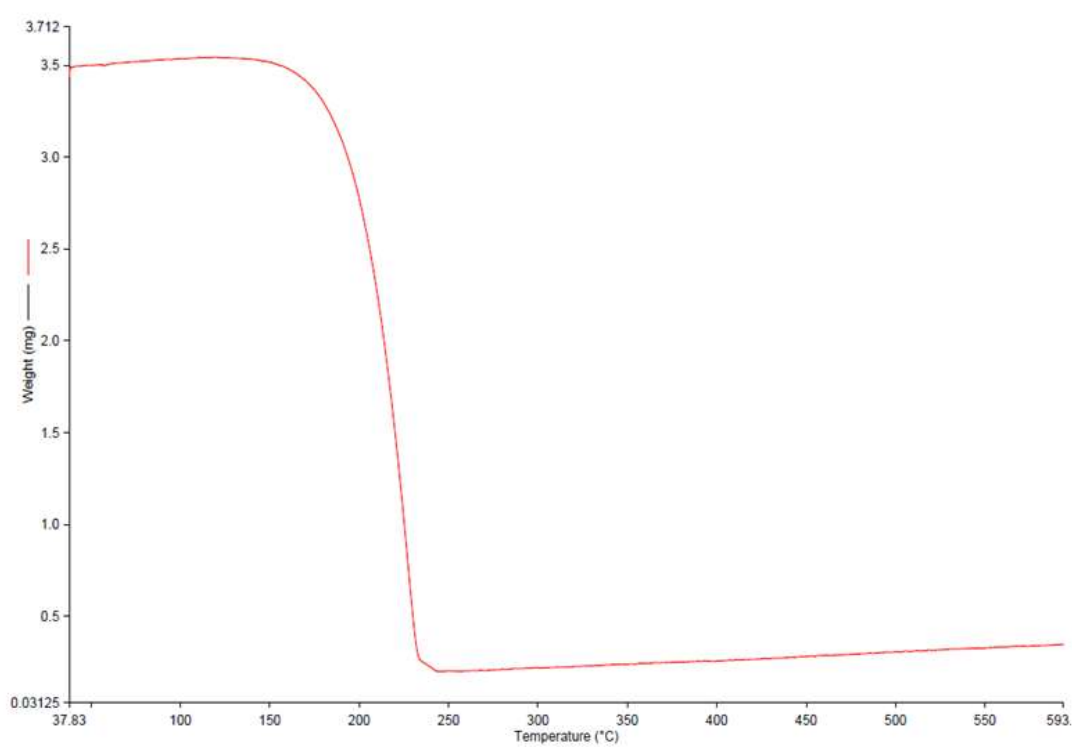
Figure 3.18 TGA curves of MA/0.5%GNP composite PCMs

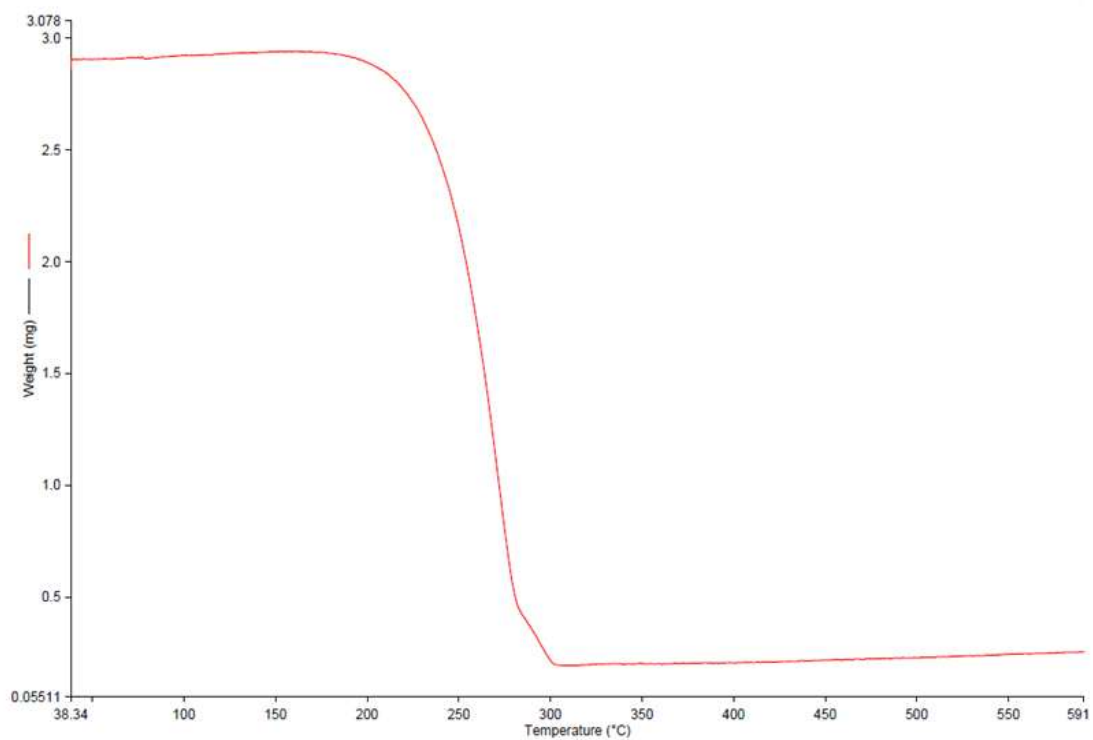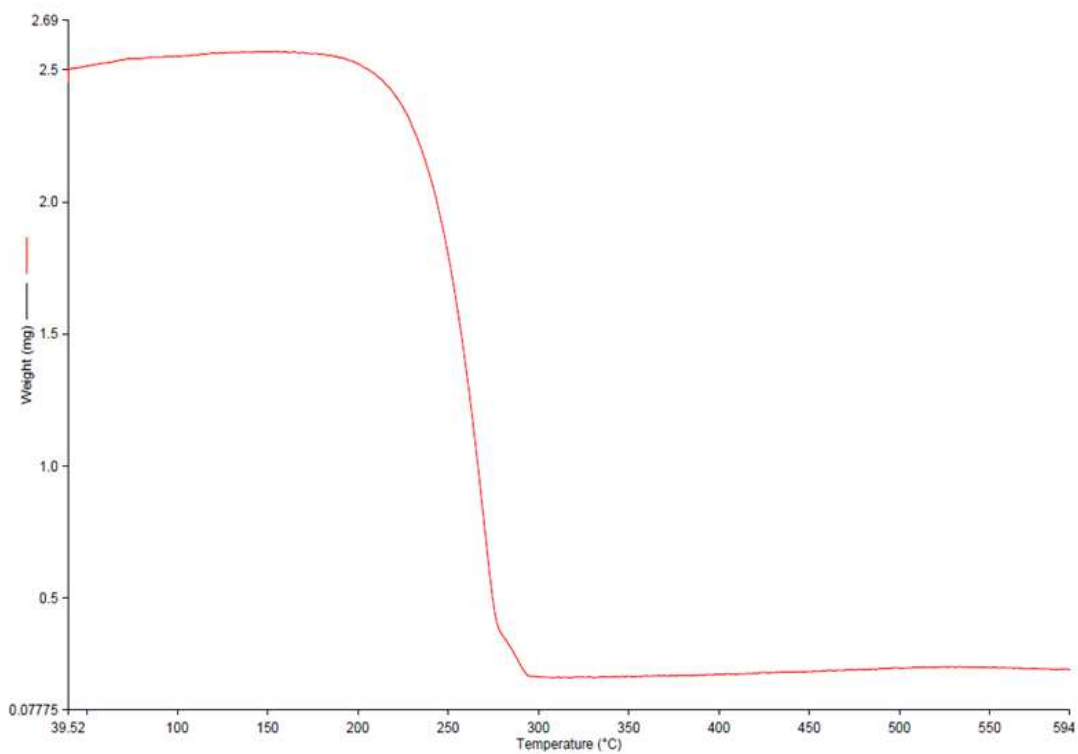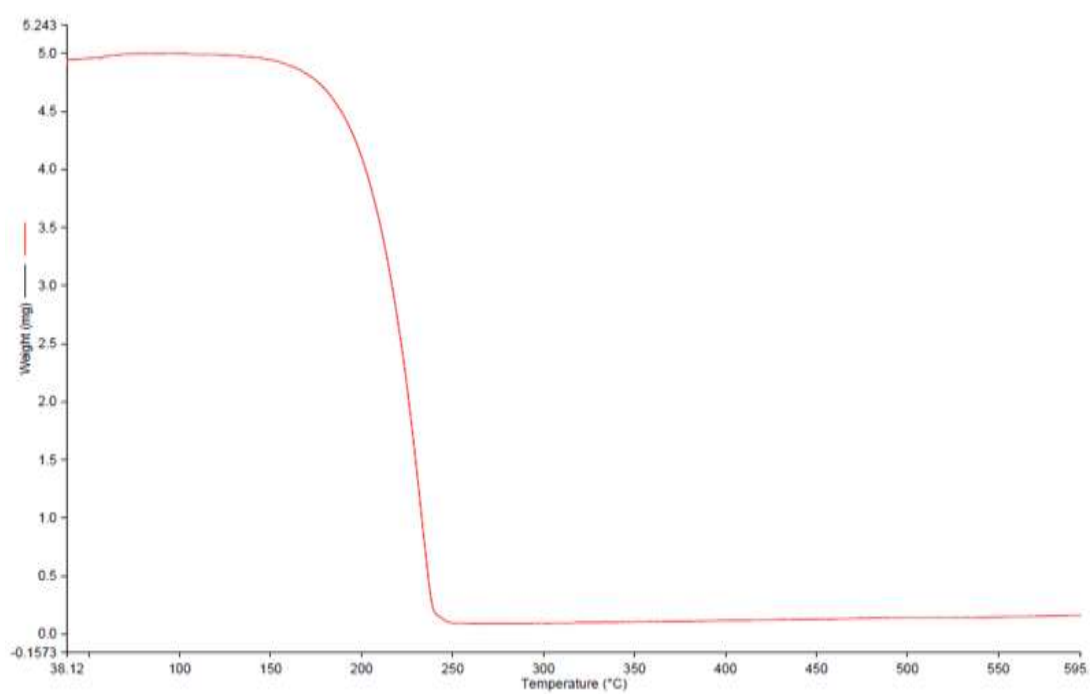Figure 3.19 TGA curves of MA/1%GNP composite PCMs
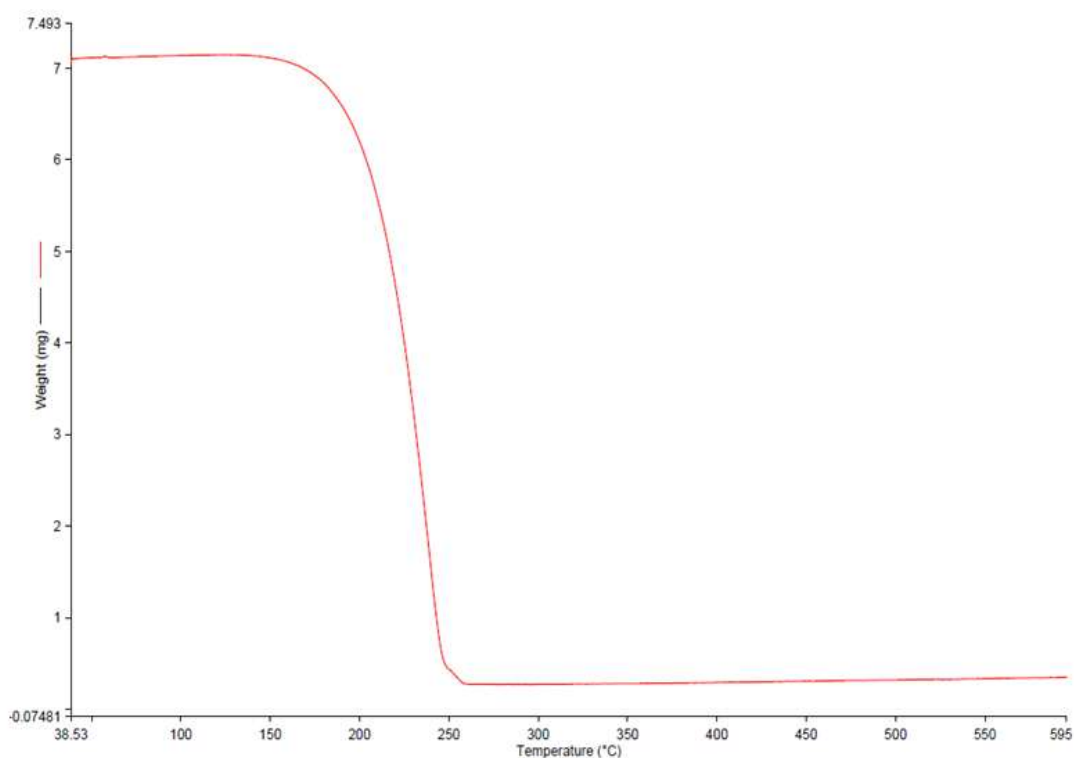
Figure 3.20 TGA curves of MA/2%GNP composite PCMs

DTG curves for AA, MA and AA/GNP, MA/GNP composite PCMs were given in Figure 3.21 and 3.22, respectively. As can be seen from the corresponding curves and data, GNP loading did not lead to considerable variations in initial degradation and maximum degradation temperatures of AA and MA. Therefore it can be stated that thermal stability of AA and MA were not affected by GNP loading at 2%/GNP loading in this study.
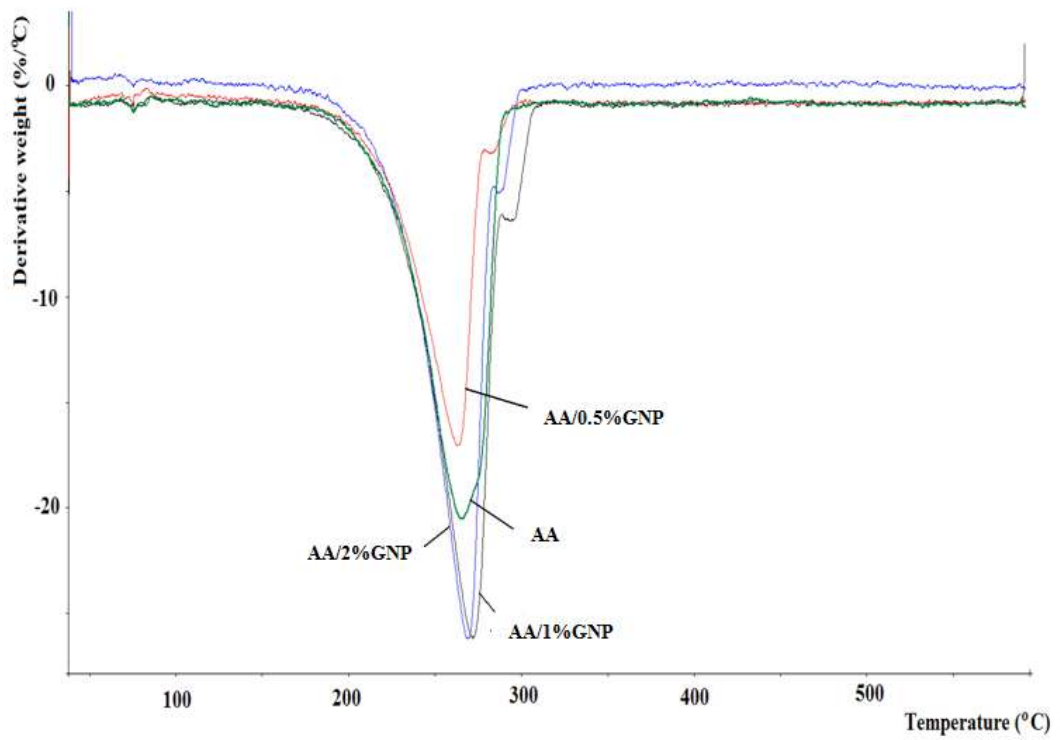
Figure 3.21 DTG curves of AA/GNP composite PCMs

Table 3.3 TGA data for AA/GNP composite PCMs

Sample	Initial (^{o}C)	End (^{o}C)	Max(^{o}C)	Weight loss to 600°C (%)
AA	178	302	265	89.2
AA/0.5% GNP	180	304	263	79.1
AA/1% GNP	173	308	272	91.1
AA/2% GNP	178	302	269	90.8
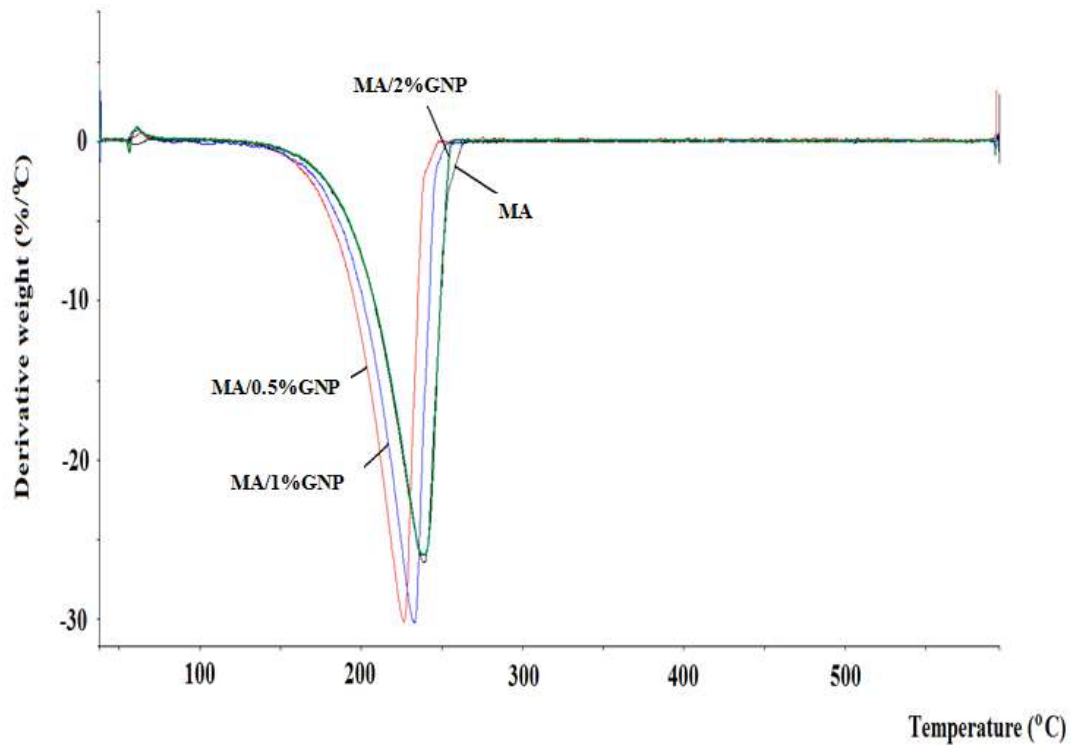
Figure 3.22 DTG curves of MA/GNP composite PCMs

Table 3.4 TGA data for MA/GNP composite PCMs

Sample	Initial (°C)	End (°C)	Max(°C)	Weight loss to 600°C (%)
MA	131	260	238	95.1
MA/0.5% GNP	125	254	227	90.0
MA/1% GNP	128	255	234	96.7
MA/2% GNP	131	262	240	95.0

3.5 Thermal Conductivity of PCMs

The thermal conductivity measurements of pure AA and AA/0.5%GNP, AA/1%GNP and AA/2%GNP composite PCMs were performed at different GNP concentrations of 0.5%, 1% and 2% wt. Thermal conductivity of pure AA was obtained to be 0.178 W/mK. Thermal conductivity values of AA/0.5%/GNP, AA/1%/GNP and AA/2%GNP was obtained to be 0.205, 0.231 and 0.254 W/mK,

42

respectively. After the GNP loading, thermal conductivity of pure AA was increased by 15%, 30% and 43% for GNP concentrations of 0.5%, 1% and 2%, respectively. These results show that there is an almost linear increasing trend with addition of the GNP particles into the pure AA.

The thermal conductivity measurements for MA and MA/GNP composite PCMs were carried out as a function of GNP loading. Thermal conductivities for MA, MA/0.5%GNP, MA/1%GNP, and MA/2%GNP PCMs were obtained to be 0.15 W/mK, 0.16 W/mK, 0.18 W/mK and 0.21 W/mK, respectively. It is clear that as the concentration of GNP loading increases, the thermal conductivity value of MA increases. Thermal conductivity of MA increased by 8%, 18% and 38%, after GNP of 0.5%, 1% and 2 % were added to MA, respectively. Even if GNP is added at low concentration (0.5%), thermal conductivity of MA increases significantly.

Fauzi et al. (2013), investigated thermal conductivity myristic acid/palmitic acid eutectic mixture with the addition of 5% sodium myristate, 5% sodium palmitate, and 5% sodium stearate surfactants. It is obtained that thermal conductivity values were determined in the range of 0.225-0.236 W/mK. Thermal conductivity of palmitic acid/expanded graphite (EG) (80/20 w/w%) composite (0.60 W/mK) was determined to be 2.5 times higher than that of pure PA (0.17 W/mK) by Sari and Karaipekli (2009). Meng and Wang (2013) prepared a PCM by using Capric acid (CA)-myristic acid (MA) eutectic as core and poly-methyl methacrylate (PMMA) as supportive matrix. When 15 wt% of modified graphite powders loaded into this PCM, thermal conductivity increased by approximately 195.9 %. Thermal conductivity of the form-stable capric acid-myristic acid/ vermiculite composite PCM was enhanced to 0.22 W/mK by adding EG of 2 wt% into the composite PCM (Sari et al., 2009).

3.6 Thermal Reliability of Composite PCMs

In order to reveal the thermal stability of composite PCMs, DSC results are presented at the end of selected number of cycles such as 10, 40, 70, and 100. The results of composites are illustrated in the following this section.

3.6.1 AA and AA/GNP composites

The superior PCM should exhibit no or less change in its thermal properties and chemical structure after long term utilization period. Therefore, thermal cycling test was performed to determine the change in thermal properties and chemical structure of the composite PCMs by DSC analysis and FTIR analysis, respectively. DSC curves of AA after 10, 40, 70 and 100 thermal cycles were shown in Figure 3.23.
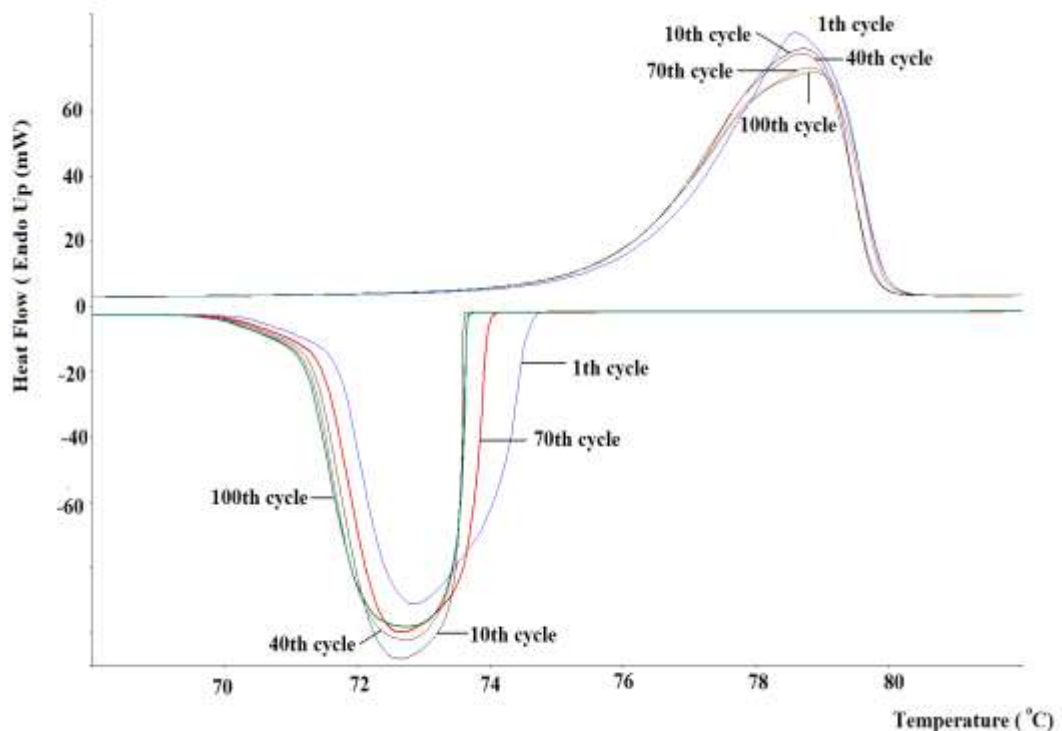

Figure 3.23 The effect of thermal cycling on thermal properties of AA

The effect of thermal cycling on thermal properties of AA, such as melting and freezing temperatures, latent heat of melting and freezing and the extent of supercooling, were presented in Table 3.5.

Table 3.5 The effect of thermal cycling on thermal properties of AA and AA/GNP composites

Sample Code	Number of thermal cycling	Melting temperature	Melting Latent heat	Freezing temperature	Freezing Latent heat	Extent of supercooling
		T_m (°C)	ΔH_m (J/g)	T_f (°C)	ΔH_f (J/g)	$T_m - T_f$ (°C)
AA	1st	76	223	75	-218	1.8
	10th	76	221	74	-218	2.4
	40th	76	220	74	-218	2.3
	70th	76	221	74	-218	1.9
	100th	76	223	74	-218	2.1
AA/0.5%GNP	1st	77.3	224	75.1	-220	2.2
	10th	76	224	75.3	-219	0.7
	40th	76	222	75.3	-218	0.7
	70th	76.1	224	75.3	-219	0.8
	100th	76	224	75.3	-219	0.7
AA/1%GNP	1st	76.2	223	75.2	-218	1.0
	10th	75.9	224	75.3	-218	0.6
	40th	75.9	224	75.3	-217	0.6
	70th	75.9	223	75.3	-217	0.6
	100th	75.9	223	75.3	-218	0.6
AA/2%GNP	1st	76.3	218	75.3	-212	1.0
	10th	75.9	217	75.4	-212	0.5
	40th	76.1	218	75.4	-213	0.7
	70th	76	217	75.4	-212	0.6
	100th	76	216	75.4	-211	0.6

The results of the AA were summarized Table 3.5. Thermal cycling did not affect the latent heat of freezing. However, after 10, 40, and 70 times of thermal cycling latent heat of melting (ΔH_m) decreased by 0.9%, 1.3%, and 0.9%, respectively. After repeated 10, 40, 70, and 100 times of thermal cycling, the freezing temperature of AA varied by -1, -1, -0.6, -0.9°C and the melting temperature varied by -0.4, -0.5, -0.5, and -0.6°C, respectively. For the case of an application of the latent thermal

energy storage, these variations are not attractive. In Table 3.5, after thermal cycling, the extent of supercooling slightly increased. It can be conclude that AA has good thermal reliability in respect to variations in phase change temperatures and latent heat values.

The effect of thermal cycling on thermal properties of AA/0.5%GNP was shown in Figure 3.24. The results derived from DSC curves of AA/0.5%/GNP were also given in Table 3.5. Except for 40th cycle, latent heat of melting did not vary after repeated thermal cycling (10, 70, and 100). At the end of 10 cycles, freezing temperature increased from 75.1 to 75.3°C and beyond that cycle it remained constant. The melting temperature of AA/0.5%GNP changed by −1.3°C after 10 cycles, −1.3°C after 40 cycles, −1.2°C after 70 cycles, and -1.3°C after 100 cycles. The freezing temperature of AA/0.5%GNP changed 0.2°C after 10 cycles, 0.2°C after 40 cycles, 0.2°C after 70 cycles, and 0.2°C after 100 cycles. The extent of supercooling for AA/0.5%GNP decreased from 2.2°C to 0.7°C after 10, 40, and 100 cycles. When AA/0.5%GNP is compared with AA in terms of the extent of supercooling, AA/0.5%GNP exhibits a better performance. After 10, 40, 70, and 100 times of thermal cycling, latent heat of freezing decreased by 0.5%, 0.9%, 0.5%, and 0.5%, respectively. AA/0.5%GNP demonstrates a good thermal reliability in respect to variations in freezing temperatures and latent heat values of melting and freezing.
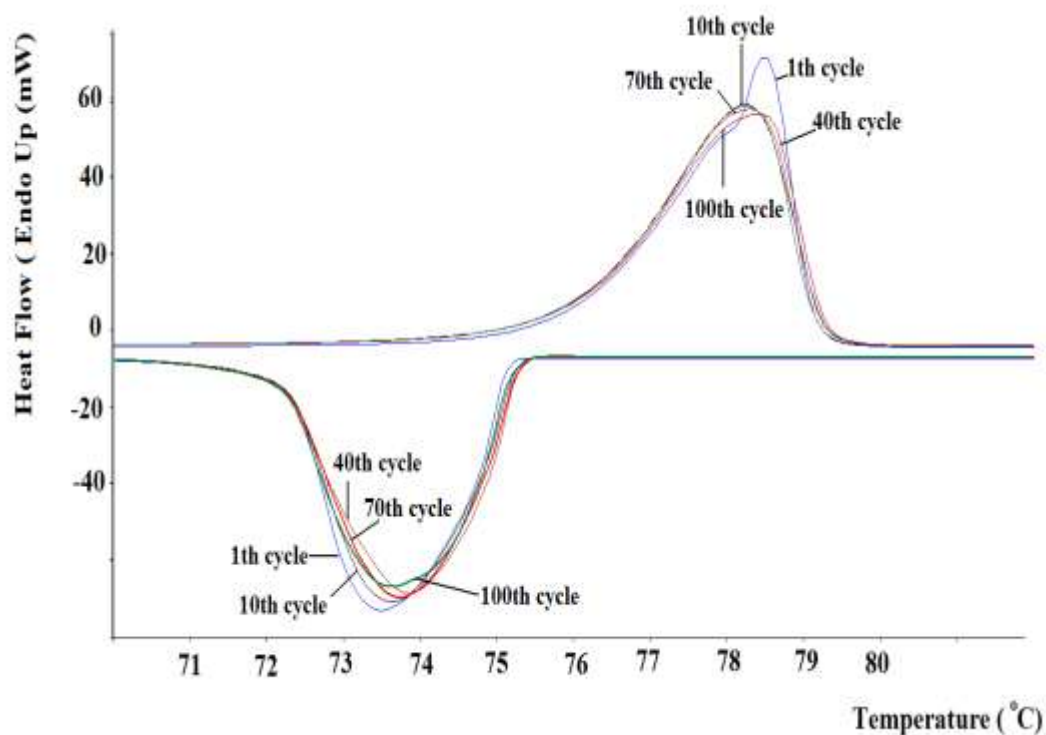
Figure 3.24 The effect of thermal cycling on thermal properties of AA/0.5%GNP

The effect of repeated thermal cycling on thermal properties of AA/1%GNP was given in Figure 3.25. The results evaluated from DSC curves of AA/1%GNP were summarized in Table 3.5. The changes in latent heat of melting and freezing of AA/1%GNP are less than 0.5% after 10, 40, 70, and 100 cycles, respectively. The melting temperatures of AA/1%GNP varied by -0.3°C after 10, 40, 70, 100 cycles. The freezing temperatures increased by 0.1°C after 10, 40, 70, and 100 cycles. The extent of supercooling decreased from 1.0°C to 0.6°C, which was superior then the pure AA and AA/0.5%GNP. In addition to this, in terms of variations in freezing temperatures, melting temperatures and latent heat values of melting and freezing, AA/1%GNP shows a better thermal reliability than AA and AA/0.5%GNP.
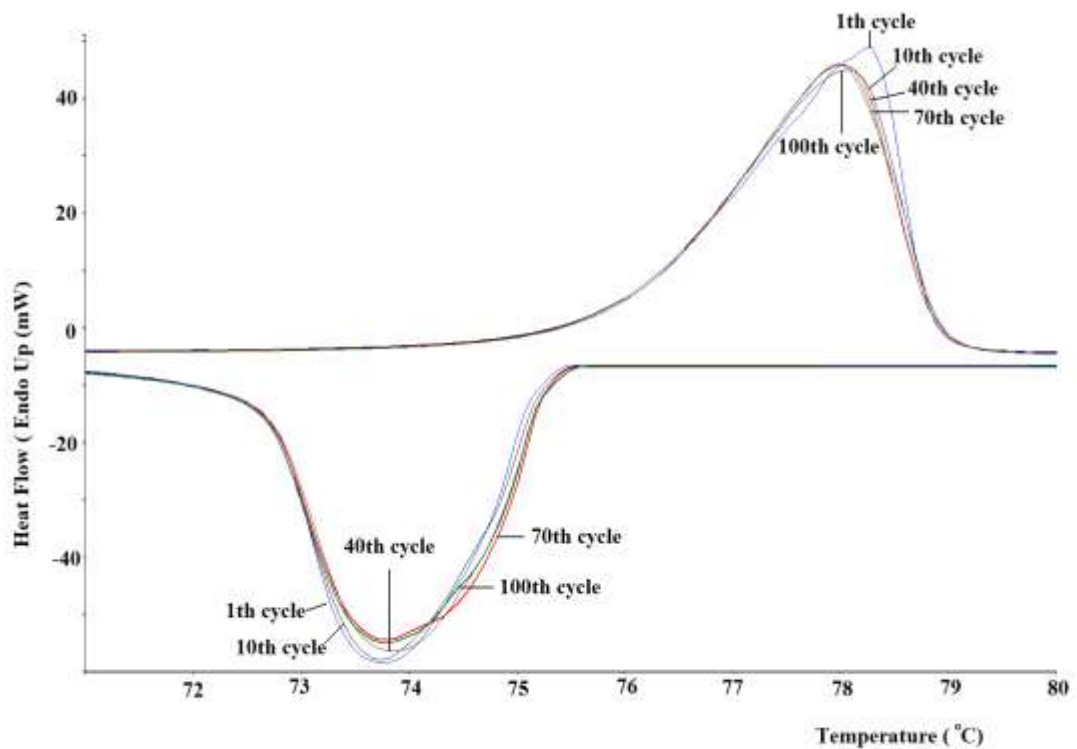
47

Figure 3.25 The effect of thermal cycling on thermal properties of AA/1%GNP

The effect of repeated thermal cycling on thermal properties of AA/2%GNP was presented in Figure 3.26. The results obtained from DSC curves of AA/2%GNP were shown in Table 3.5. The melting temperature of AA/2%GNP changed by -0.4°C, -0.2°C, -0.3°C, and -0.3°C after 10, 40, 70, and 100 cycles, respectively. However, freezing temperature of AA/2%GNP increased by 0.1°C after 10, 40, 70, and 100 cycles. Melting and freezing latent heat values are changed by less than 1% after repeated thermal cycles. As can be seen from Table 3.5, the extent of supercooling decreased after repeated thermal cycling. In terms of variations in phase change temperatures and latent heat values of melting and freezing, AA/2%GNP exhibits a good thermal reliability.
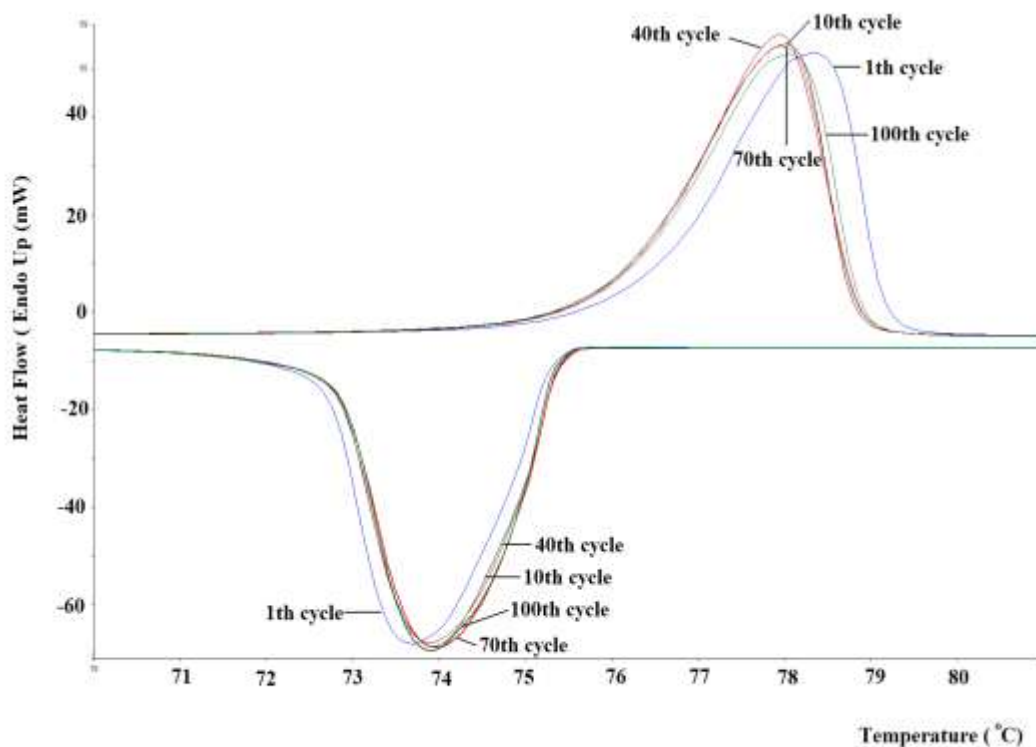
Figure 3.26 The effect of thermal cycling on thermal properties of AA/2%GNP

3.6.2 MA and MA/GNP Composites

The effect of thermal cycling on thermal properties of MA was given in Figure 3.27. The results were summarized in Table 3.6. The melting temperature of MA decreased by 0.3°C for all number of thermal cycling, but the freezing temperature of MA increased by 0.2, 0.3, 0.4 and 0.6°C after 1, 10, 40, 70 and 100 times of thermal cycling of MA. On the other hand, melting and freezing latent heat values decreased by 4 J/g after 100 times of thermal cycling of MA. It can be noted that these variations can be considered as fairly small variations. The extent of supercooling decreased with the increasing of thermal cycling number, from 2.3°C (first cycle) to 1.4°C (100th cycle).
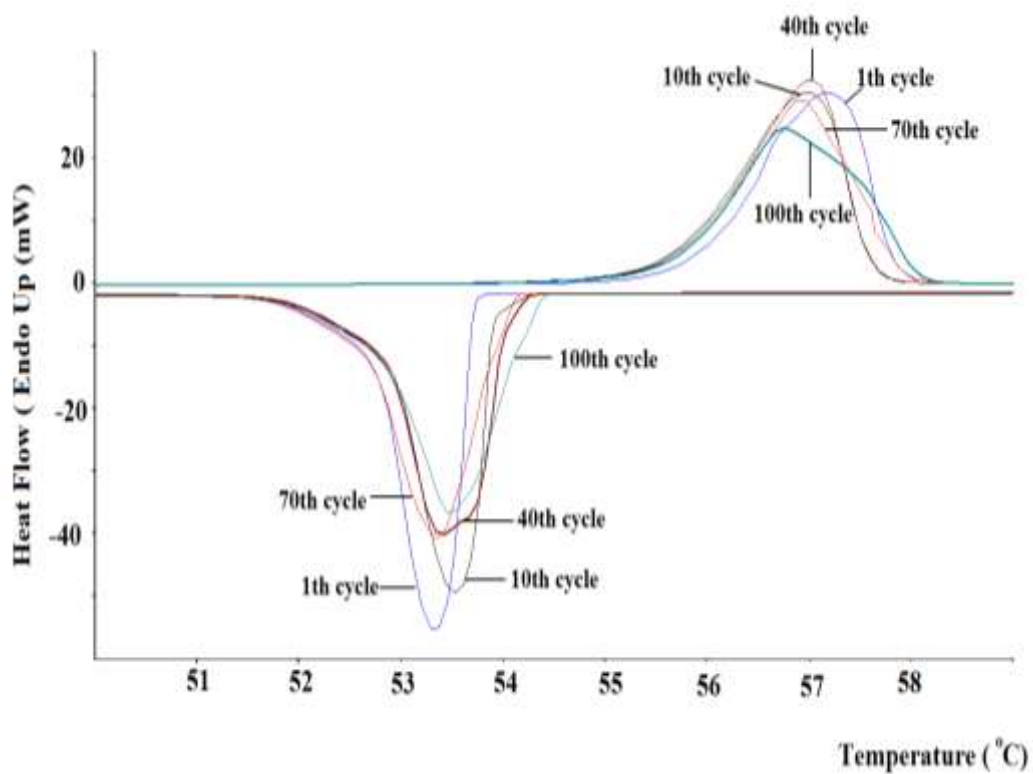
Figure 3.27 The effect of thermal cycling on thermal properties of MA

Table 3.6 The effect of thermal cycling on thermal properties of MA and MA/GNP composites

Sample Code	Number of thermal cycling	Melting temperature	Melting Latent heat	Freezing temperature	Freezing Latent heat	Extent of supercooling
		T_m (°C)	ΔH_m (J/g)	T_f (°C)	ΔH_f (J/g)	T_m - T_f (°C)
MA	1st	56.0	202	53.7	-196	2.3
	10th	55.7	200	53.9	-194	1.8
	40th	55.7	200	54.0	-193	1.7
	70th	55.7	198	54.1	-193	1.6
	100th	55.7	198	54.3	-192	1.4
MA/0.5%GNP	1st	56.0	196	54.8	-195	1.2
	10th	55.7	197	54.8	-194	0.9
	40th	55.7	197	54.9	-193	0.8
	70th	55.7	197	54.9	-193	0.8
	100th	55.7	197	54.9	-193	0.8
MA/1%GNP	1st	54.8	183	53.7	-182	1.1
	10th	54.7	186	53.8	-182	0.9
	40th	54.7	186	53.8	-182	0.9
	70th	54.7	186	53.8	-181	0.9
	100th	54.7	186	53.8	-181	0.9
MA/2%GNP	1st	54.6	186	53.7	-182	0.9
	10th	54.7	185	53.7	-180	1.0
	40th	54.7	185	53.7	-180	1.0
	70th	54.7	184	53.7	-180	1.0
	100th	54.7	184	53.7	-180	1.0

The effect of the number of thermal cycling on melting and freezing temperatures, latent heat values of melting and freezing temperatures and the extent of supercooling of MA/0.5%GNP composite was shown in Table 3.6. DSC curves for cycled MA/0.5%GNP composite PCM at various cycles were given in Figure 3.28.

As can be seen from Table 3.6, latent heat values of melting and freezing remained similar after thermal cycling of MA/0.5%GNP composite. Melting temperature of MA/0.5%GNP decreased from 56.0 to 55.7°C after 10 thermal cycles and remained unchanged as the number of cycle increases. Freezing temperature of MA/0.5%GNP seems to be almost the same after thermal cycling process up to 100

times. Cycled MA/0.5%GNP composite led to better result in terms of the extent of crystallinity when compared to cycled MA. As a conclusion, when we compare the MA/0.5%GNP composite PCM with the pure MA, MA/0.5%GNP has a better thermal reliability during thermal cycles.
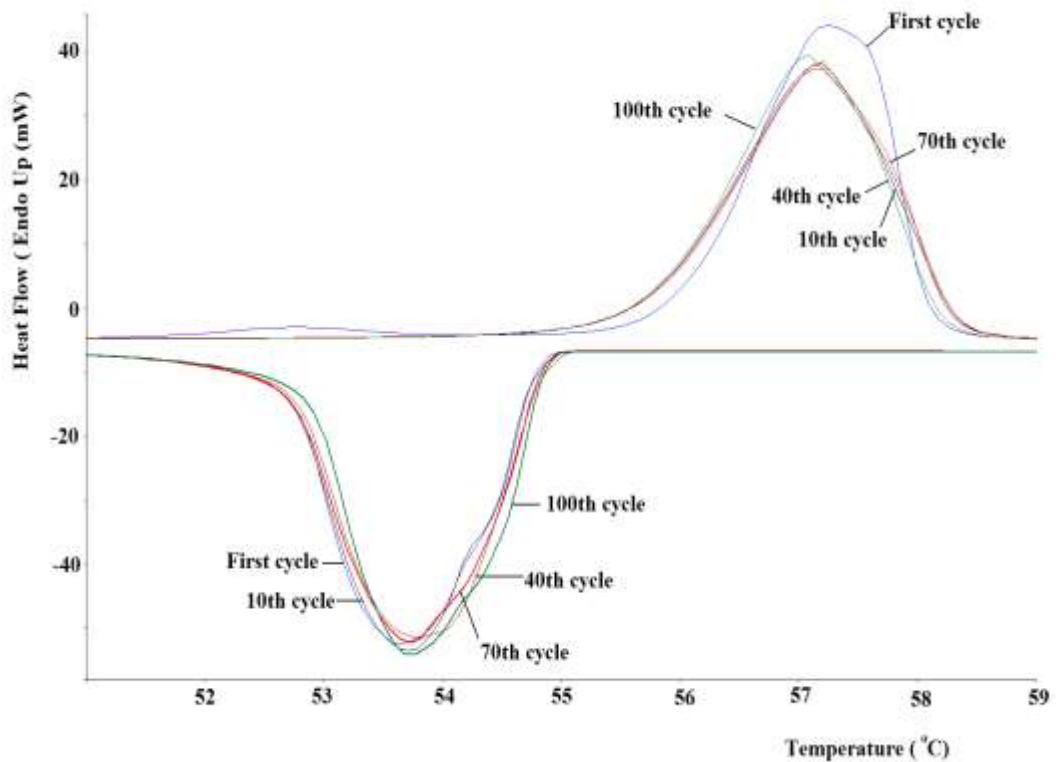

Figure 3.28 The effect of thermal cycling on thermal properties of MA/0.5%GNP

DSC curves of cycled MA/1%GNP composite PCM were presented in Figure 3.29. Thermal properties of MA/1%GNP at various numbers of thermal cycles were summarized in Table 3.6. While melting temperatures of MA/1%GNP decrease by 0.1°C after 10 cycles, freezing temperatures increased by 0.1°C after 10 cycles. At higher cycles (40, 70 and 100) melting and freezing temperatures remained the same. Besides, there is no significant variation in the latent heat of freezing. However latent heat of melting increased from 183 J/g to 186 J/g after 10 cycles. Increasing the number of cycles does not cause any significant change in terms of melting latent heat. The extent of supercooling of MA/1%GNP decreased by 0.2°C after 10 thermal cycles and for the remaining cycles, no change has been observed in terms of the

degree of supercooling. In the light of these results, MA/1%GNP possesses a good thermal stability as well as MA/0.5%GNP.
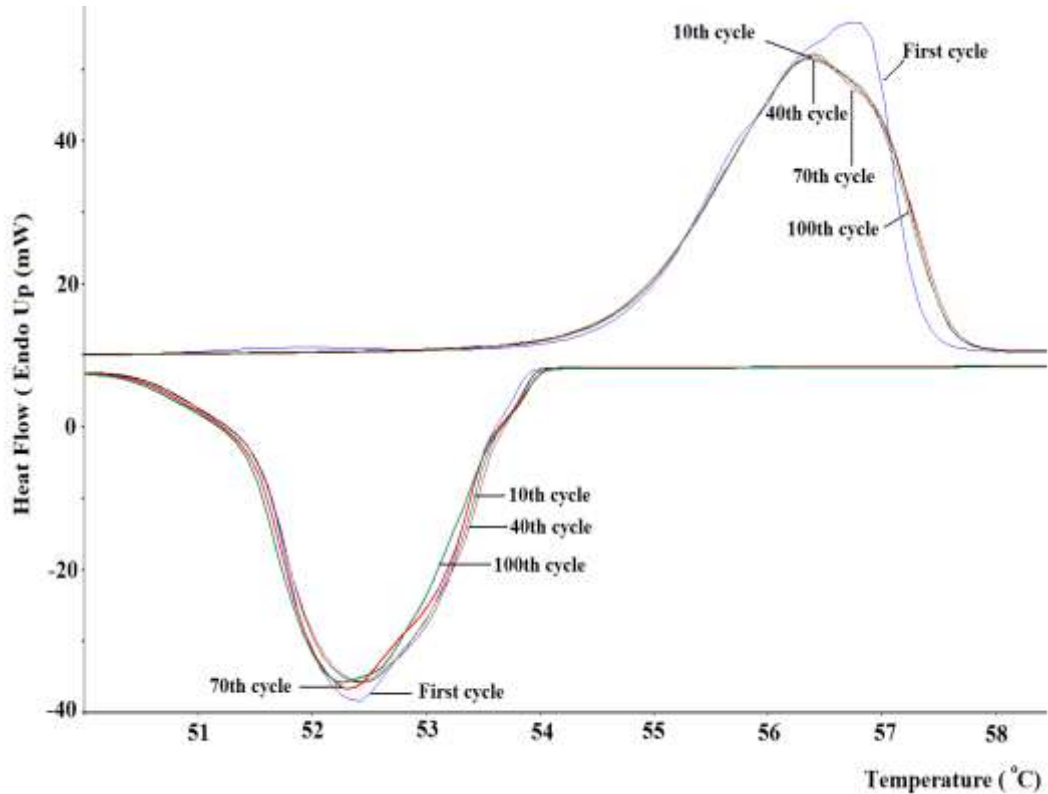

Figure 3.29 The effect of thermal cycling on thermal properties of MA/1%GNP

DSC curves of cycled MA/2%GNP composite PCM were shown in Figure 3.30 The effect of number of thermal cycling on thermal properties of MA/2%GNP was summarized in Table 3.6. It is interesting to state that freezing temperature of MA/2%GNP did not change after thermal cycling process even at the highest cycle number (100). Melting temperature was raised by 0.1°C after 10 cycles and remained the same at higher cycle numbers. Latent heat values of melting and freezing decreased by 2 J/g after 100 cycles. The extent of supercooling was calculated to be 1°C after 10, 40, 70 and 100 cycles. Considering the above-stated thermal properties, one can conclude that MA/2%GNP shows a good thermal stability upon thermal cycling.
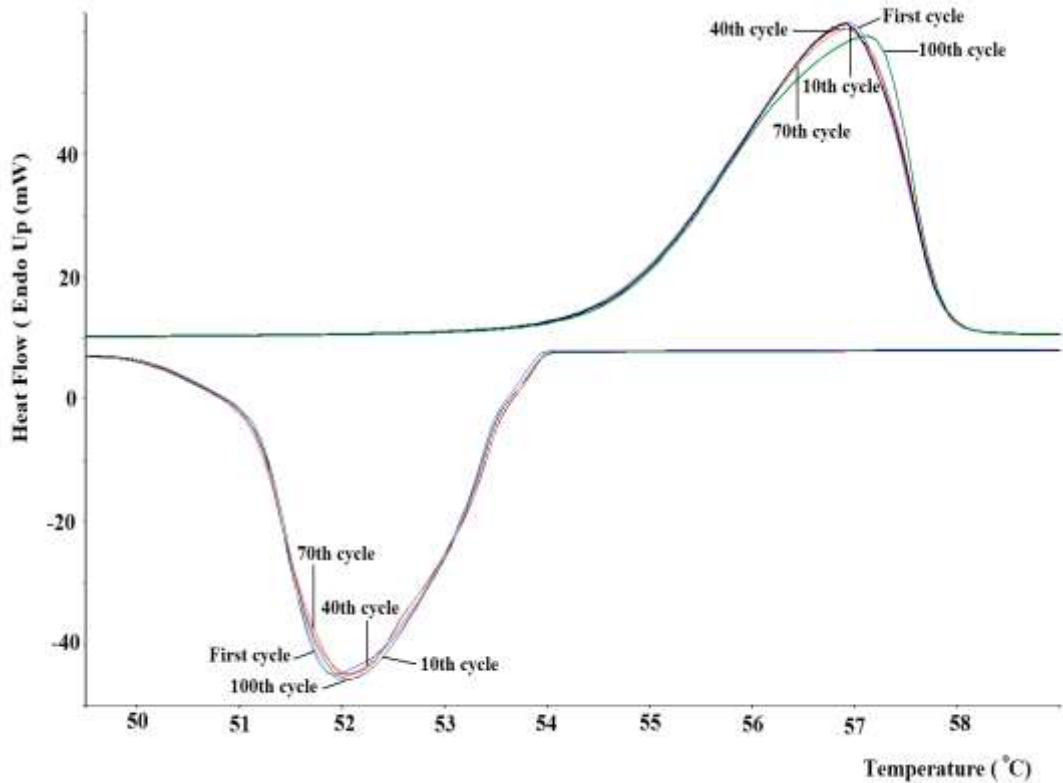
Figure 3.30 The effect of thermal cycling on thermal properties of MA/2%GNP

3.7 The Effect of Cycling Process on Chemical Stability of PCMs

The chemical stability of AA after various numbers of thermal cycles was found out by FTIR analysis. FTIR spectra of thermally cycled AA, AA/0.5%GNP, AA/1%GNP and AA/2%GNP were shown in Figures 3.31, 3.32, 3.33, and 3.34, respectively. As can be seen from Figure 3.31, FTIR spectra of un-cycled and cycled AA are almost the same.

It can be seen that repeated melting-freezing cycles did not cause degradation in chemical structure of AA. It can be noted that AA is stable in chemically after 100 times of thermal cycling. However, Figures 3.32, 3.33 and 3.34 demonstrate that FTIR spectra of thermally cycled GNP based composite PCMs are almost the same as un-cycled counterpart except for disappearance of the band at about 1431 cm^{-1}, especially for the samples of AA/1%GNP and AA/2%GNP, which corresponds to CH2 groups of AA. It can be seen that 100 times of thermal cycling do not lead to significant variation in chemical stability of AA/GNP composites.
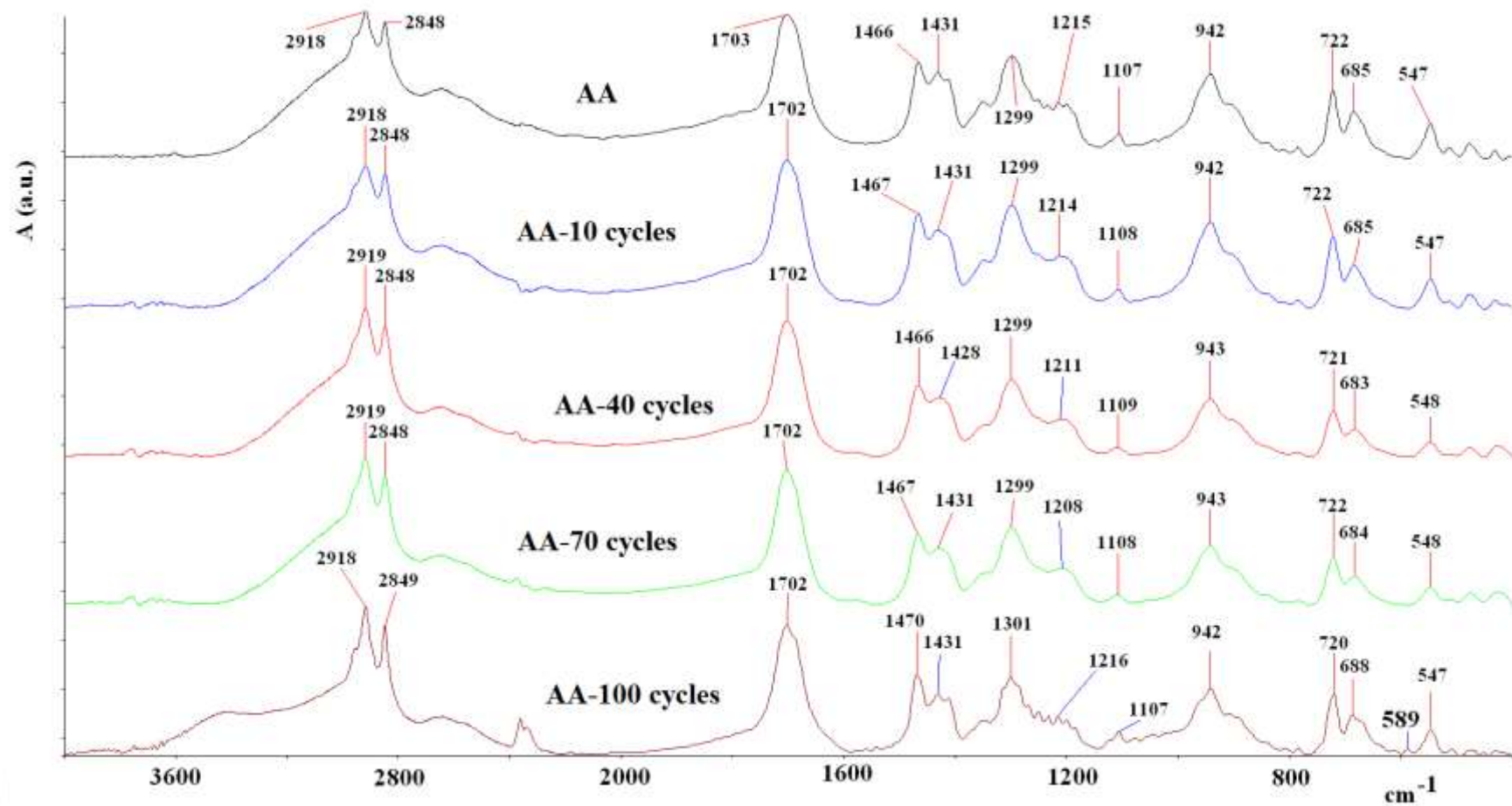
Figure 3.31 The effect of thermal cycling on functional groups of AA
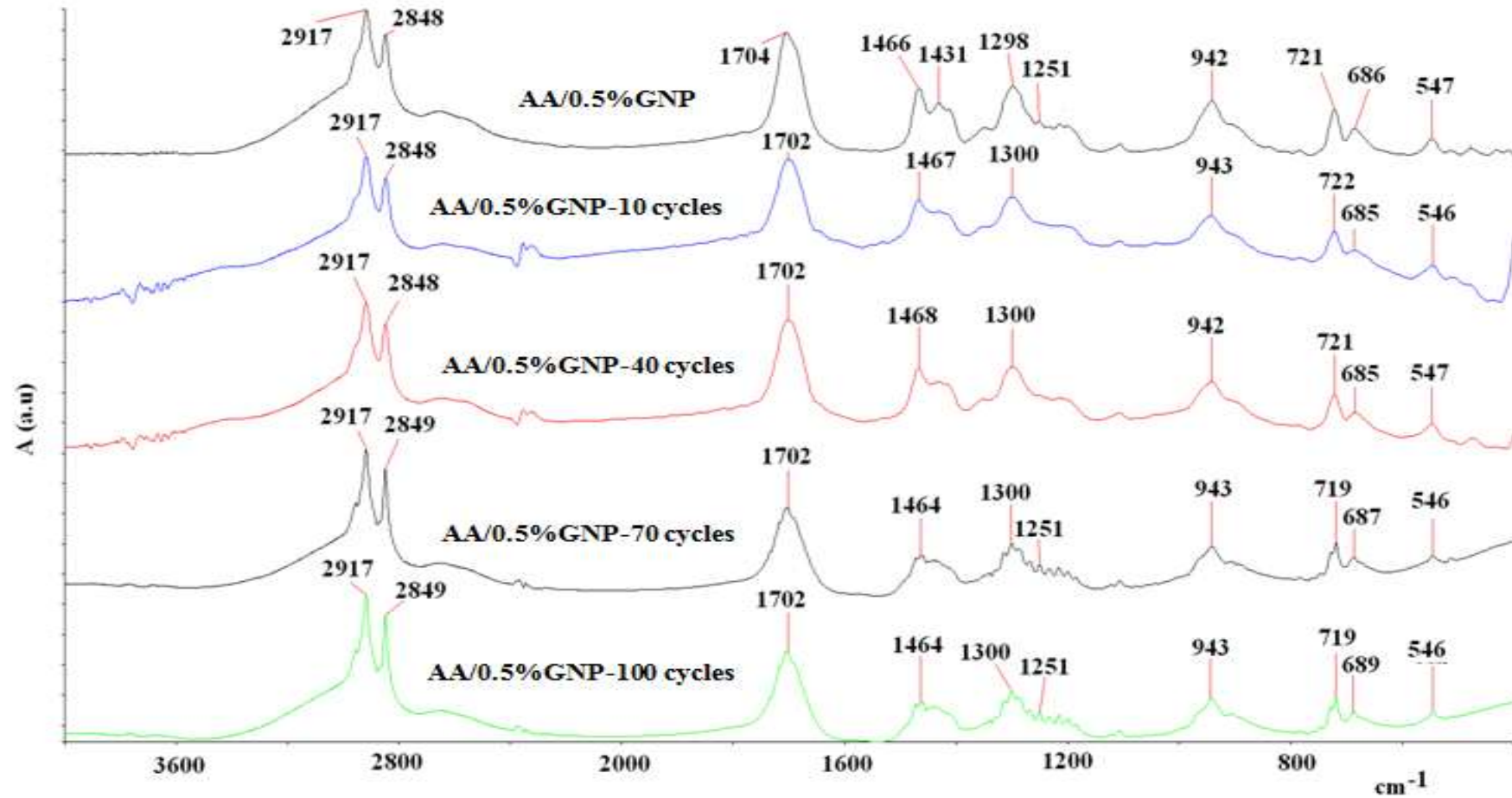
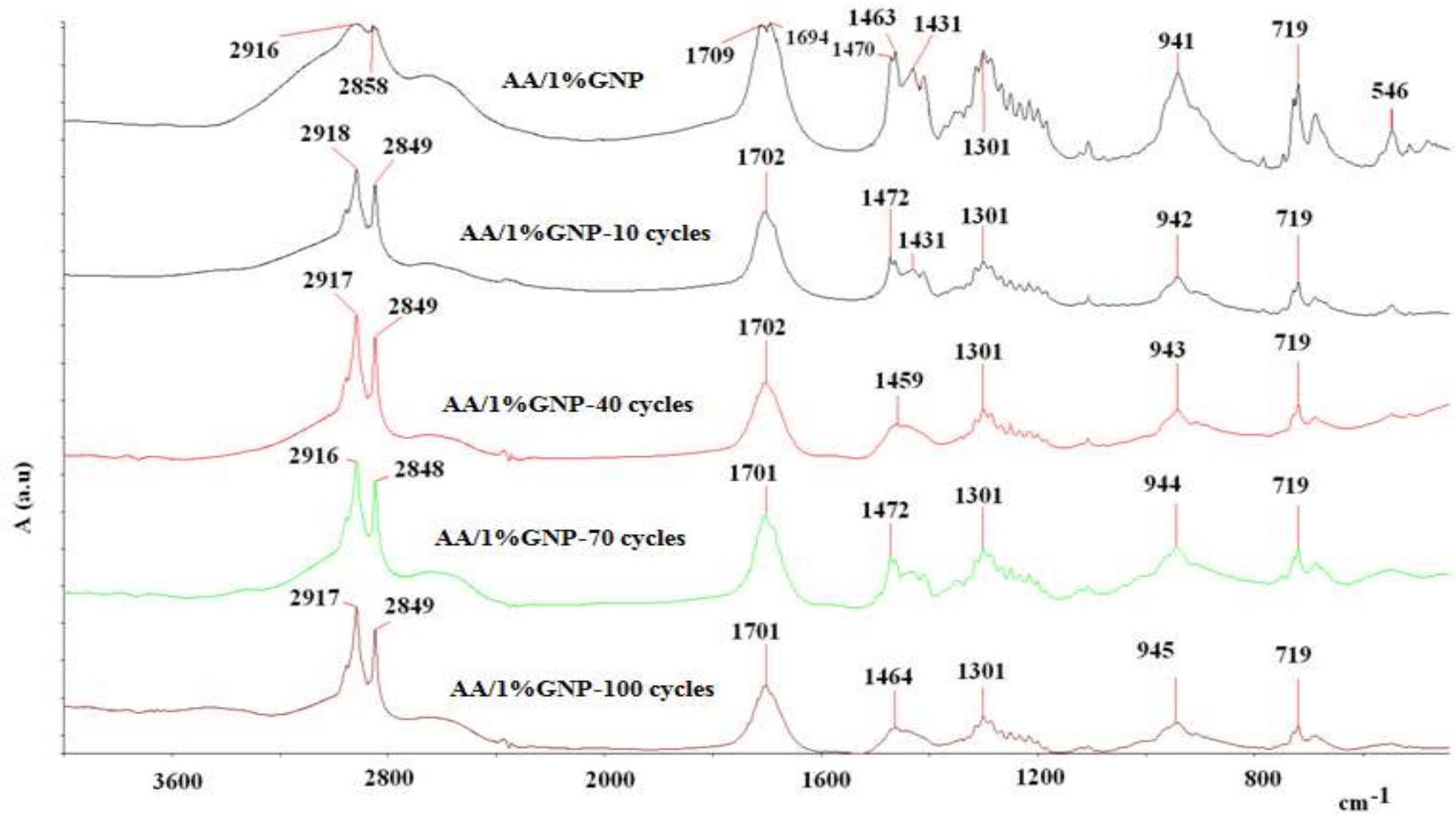Figure 3.32 The effect of GNP loading on functional group of AA/0.5%GNP.

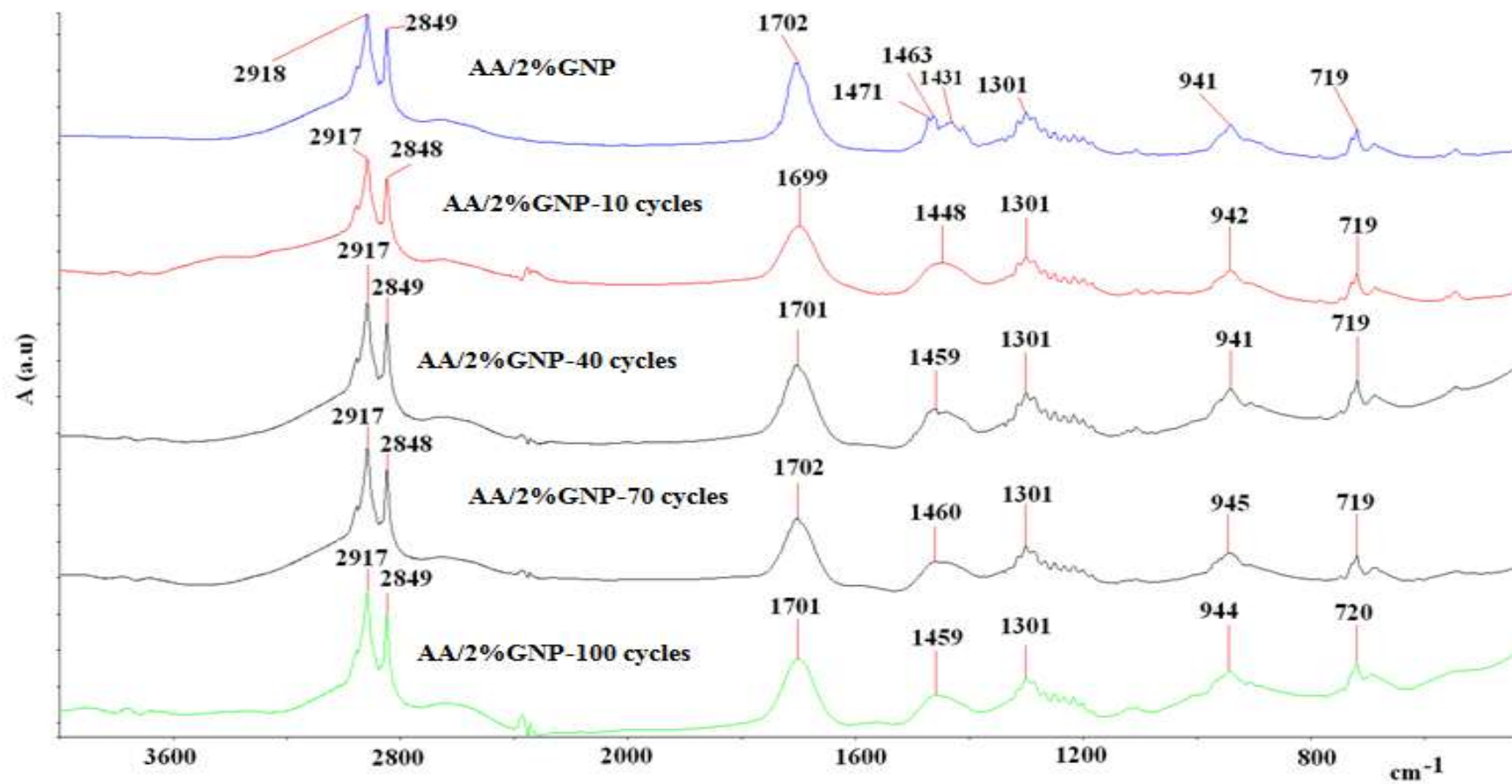Figure 3.33 The effect of GNP loading on functional group of AA/1%GNP

Figure 3.34 The effect of GNP loading on functional group of AA/2%GNP

The effect of thermal cycling on functional groups of MA, MA/0.5%GNP, MA/1%GNP and MA/2%GNP were shown in Figures 3.35, 3.36, 3.37 and 3.38. FTIR spectra of cycled MA samples remained the same with that of MA due to which it is reported that repeated melting-freezing cycles do not lead any deterioration in chemical stability of MA. In Figure 3.36, it can be seen that, thermal cycling test does not make any significant change on functional groups of MA/0.5%GNP. Therefore, one can conclude that MA/0.5%GNP remained stable in chemically after 100 times of thermal cycling.

When the FTIR spectra of MA/1%GNP at various thermal cycles were compared, it is seen that after 100 cycles some small bands, for example about 1200 cm^{-1}, disappears and a new band appears at 1579 cm^{-1}. This band may be attributed to an asymptotic response of the carboxylate absorption at 1573 cm^{-1}. Except for 100 cycles, MA/1%GNP shows fairly good chemical stability upon thermal cycling.

FTIR spectrum of MA/2%GNP is more close to the spectra of 40 and 70 cycles, which indicates less variation in chemical stability. It is probable that, when GNP of 2% is used to make composite, GNP may not be properly dispersed in molten MA.
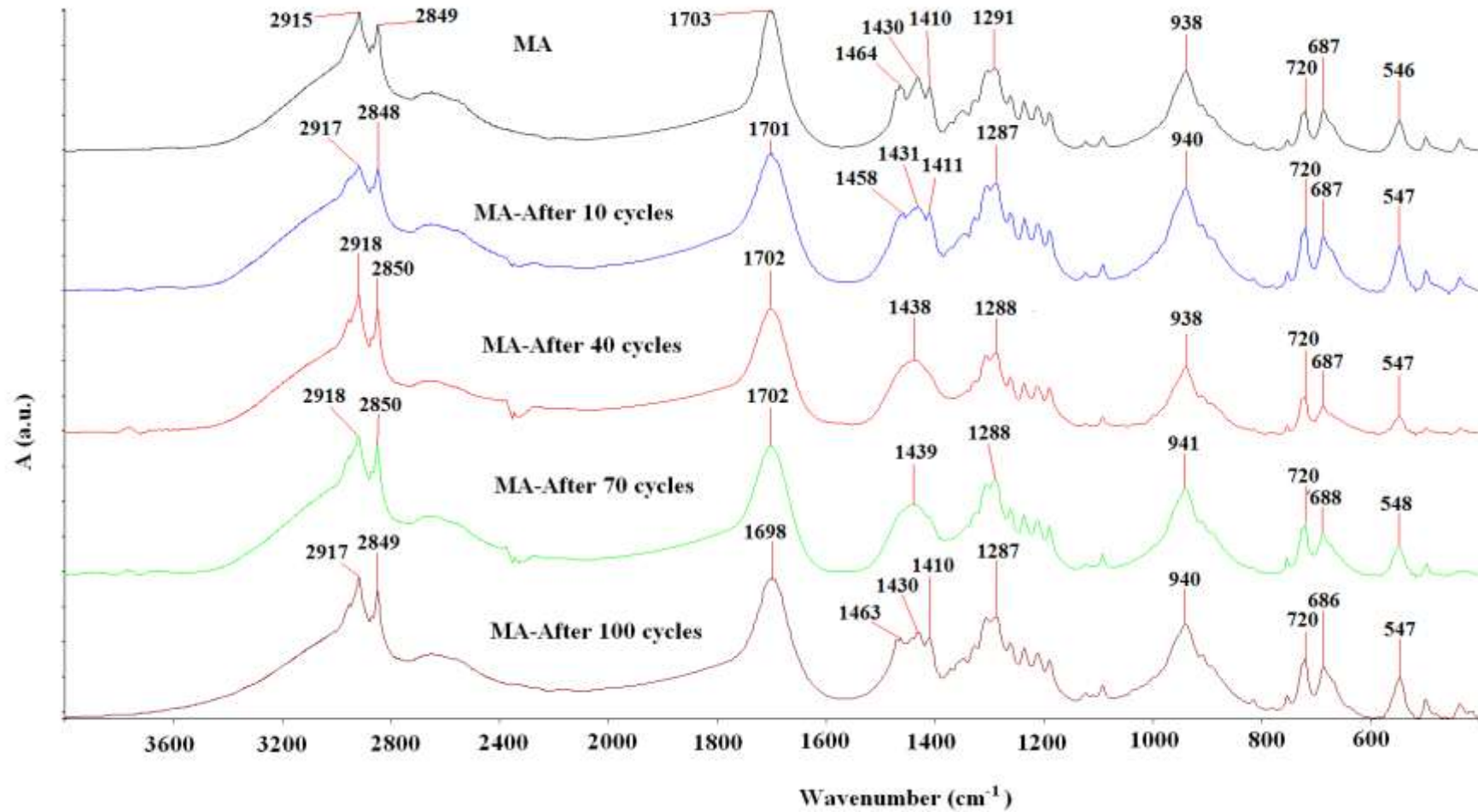
Figure 3.35 The effect of thermal cycling on functional groups of MA
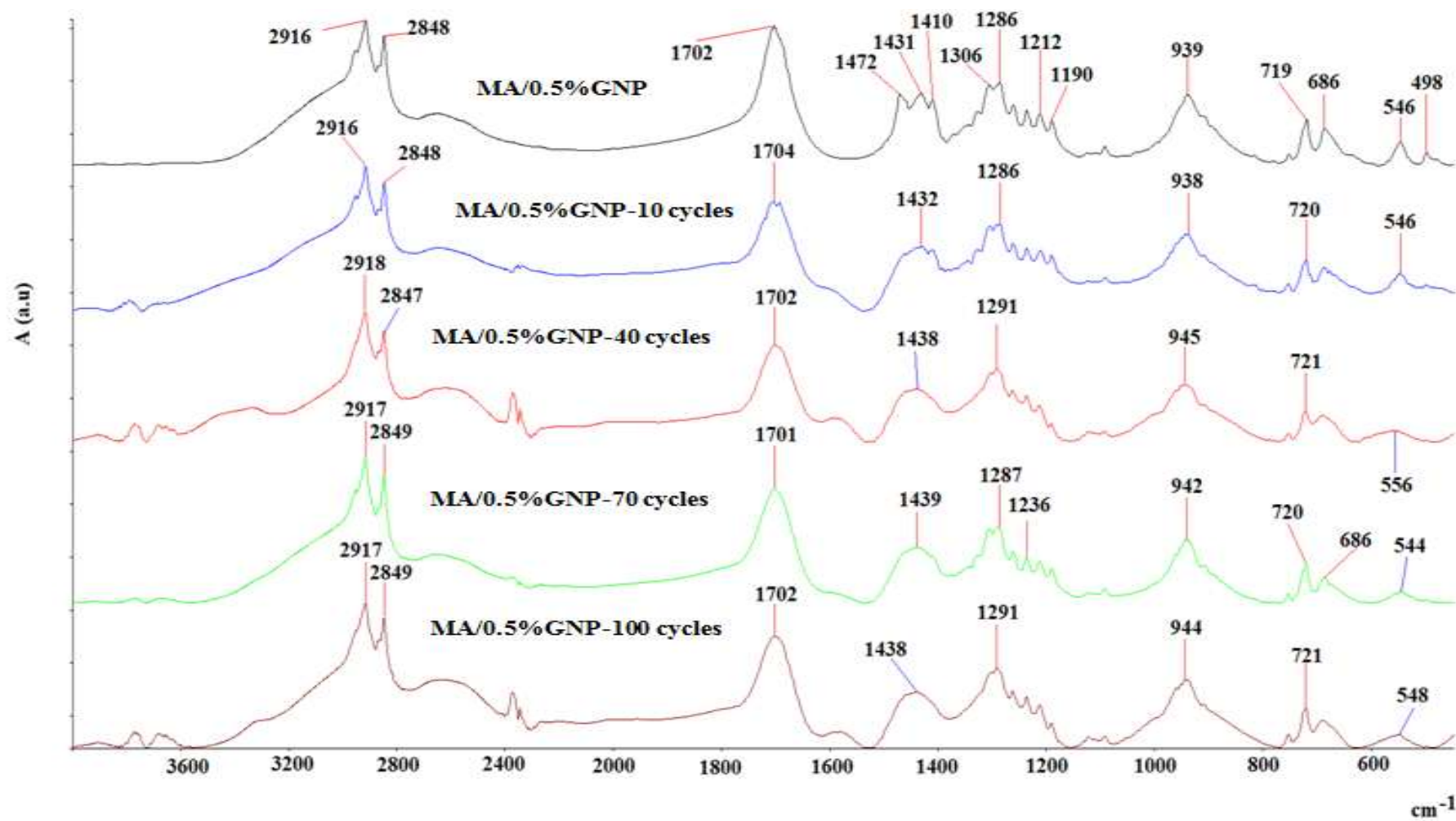
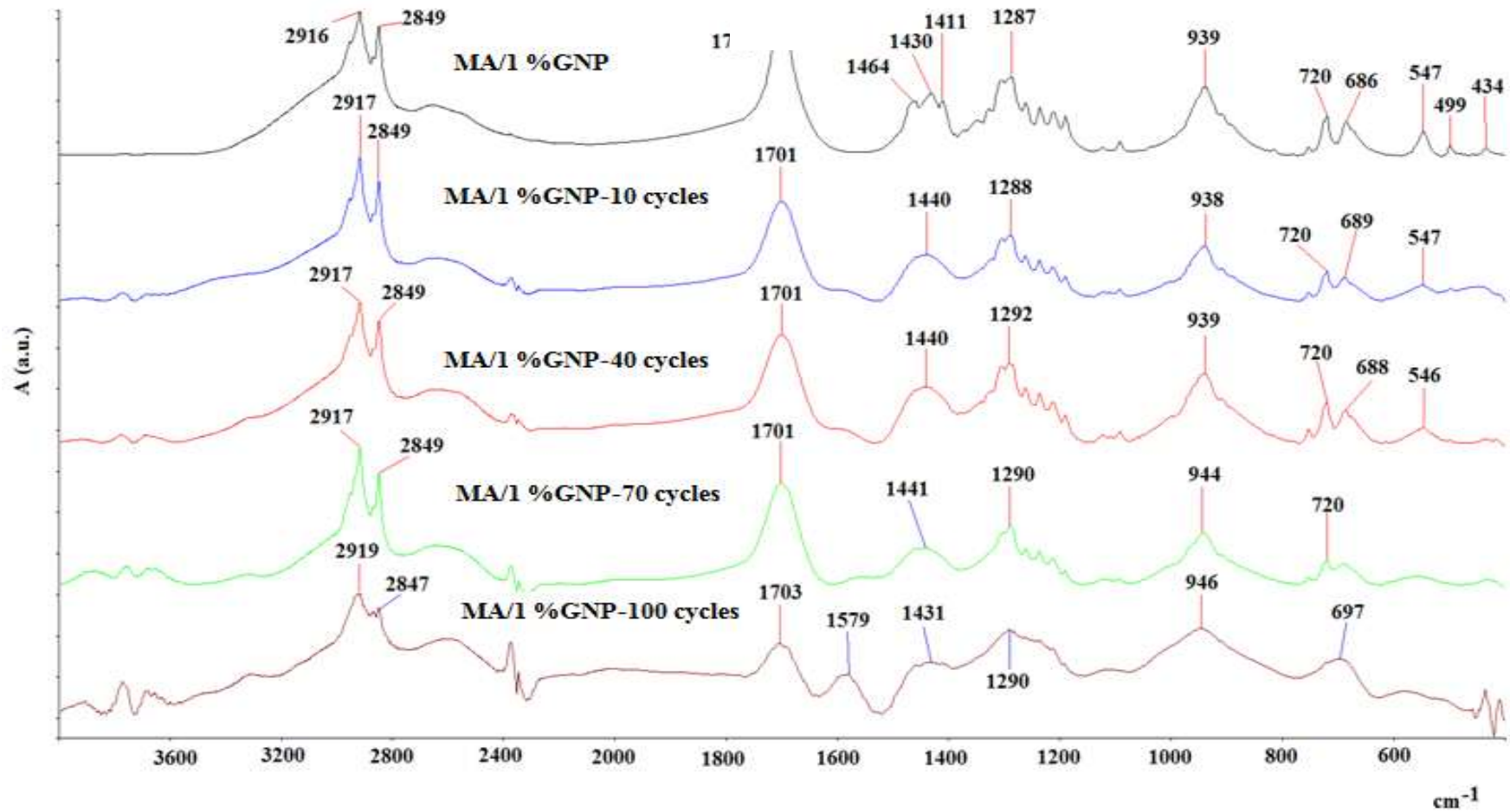Figure 3.36 The effect of GNP loading on functional group of MA/0.5%GNP

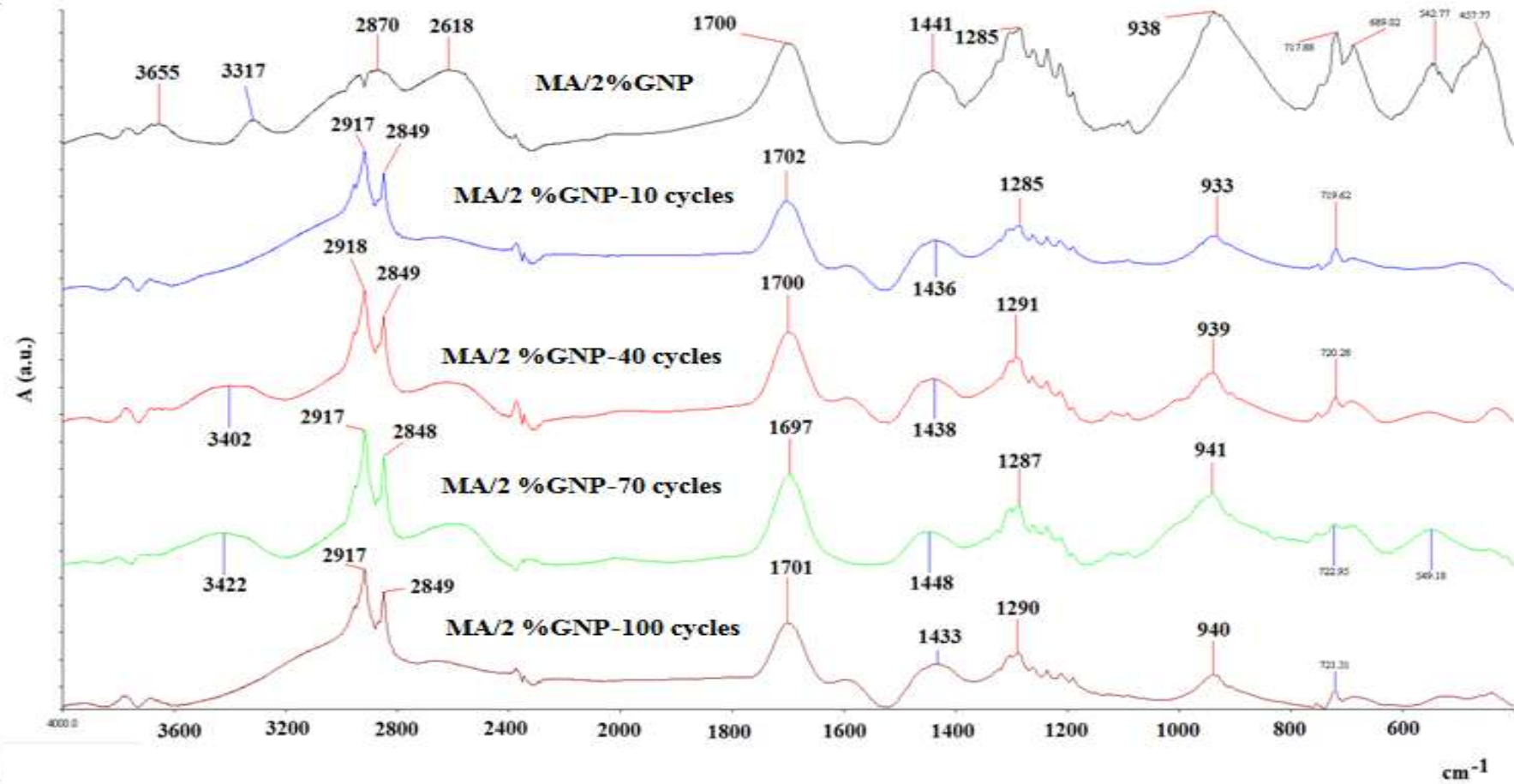Figure 3.37 The effect of GNP loading on functional group of MA/1%GNP

Figure 3.38 The effect of GNP loading on functional group of MA/2%GNP

CHAPTER FOUR
CONCLUSIONS

Since the duration of charging and discharging periods are limited for solar power, it is critical to finalize the process in a pre-determined time period. This study mainly focuses on increasing the thermal conductivity of a PCMs (Arachidic acid and Myristic acid) which are suitable for moderate temperatures such as solar energy applications. In conclusion, two different samples were examined for thermal and chemical characteristics of PCMs with GNP loading. AA/GNP and MA/GNP composites PCMs were successfully fabricated in this study.

Latent heat of fusion (220 J/g) and the phase change temperature (73°C) of the pure Arachicid Acid is suitable for solar power systems. GNP loading tends to decrease the effect of sub-cooling and ensures stable and reliable PCM even for the long term utilizations. Thermal conductivity of pure AA was enhanced by 15%, 30% and 43% for GNP concentrations of 0.5%, 1% and 2%, respectively. Results emphasizes that discharging or charging process in a latent heat thermal energy system could be optimized by selecting appropriate amount of GNP loading to regulate heat transfer speed in the system.

GNP loading did not lead to considerable variations in initial degradation and maximum degradation temperatures of myristic acid. Thermal conductivity of MA increased by 8%, 18% and 38%, after GNP of 0.5%, 1% and 2% was added to MA, respectively. From FTIR analysis, relatively weak chemical interactions between GNP and MA were observed. GNP loading did not affect considerably the melting and freezing temperatures, latent heats of melting and freezing of MA. However the extent of crystallinity remained the same and the extent of super-cooling of MA was decreased from 2.5°C to 0.7°C. After thermal cycles of 10, 40, 70 and 100 significant variations was not observed in thermal properties and chemical stability of MA. It can be reported that MA/GNP composite PCM, especially MA/0.5%GNP and MA/1%GNP, have a better thermal reliability during thermal cycles than that of MA.

Thermal cycling results also proved that proposed composite PCMs are suitable for long term utilization.

Current findings reveal that GNP loadings in AA and MA, even for smallest amounts, tend to increase the thermal conductivity of composite PCM and reduce the total phase change time without any significant change in the remaining thermal properties, such as phase change temperature or latent heat. In contrary, it is introduced that the GNP loading decreases the degree of sub-cooling. Thermal cycling results also proved that proposed composite PCMs are suitable for long term utilization.

REFERENCES

Abhat, A. (1983). Low temperature latent heat thermal energy storage: heat storage materials. *Solar energy*, *30*(4), 313-332.

Ashrae, H. (1999). Applications Handbook. *American Society of Heating, Ventilating.*

Dincer, I., & Rosen, M. (2002). *Thermal energy storage: systems and applications*. John Wiley & Sons.

Erek, A., & Ezan, M. A. (2011). Experimental investigations on the thermal properties of the phase change materials and heat transfer fluıds used in the thermal energy storage systems. *Dokuz Eylül University Faculty of Engineering Mechanical Engineering* SRP Bid Report (2008.KB. FEN.33)

Ezan, M. A. (2011). *Experimental and numerical investigation of cold thermal energy storage systems.* PhD Thesis, Dokuz Eylül University, İzmir.

Fang, G., Li, H., Chen, Z., & Liu, X. (2010). Preparation and characterization of stearic acid/expanded graphite composites as thermal energy storage materials. *Energy*, *35*(12), 4622-4626.

Farid, M. M., Khudhair, A. M., Razack, S. A. K., & Al-Hallaj, S. (2004). A review on phase change energy storage: materials and applications. *Energy Conversion and Management*, *45*(9), 1597-1615.

Fauzi, H., Metselaar, H. S., Mahlia, T. M. I., Silakhori, M., & Nur, H. (2013). Phase change material: optimizing the thermal properties and thermal conductivity of myristic acid/palmitic acid eutectic mixture with acid-based surfactants. *Applied Thermal Engineering*, *60*(1), 261-265.

Ferreira, M., Wohnrath, K., Riul, A., Giacometti, J. A., & Oliveira, O. N. (2002). Interactions at the molecular level between biphosphine ruthenium complexes and stearic acid in Langmuir and Langmuir-Blodgett films. *The Journal of Physical Chemistry B*, *106*(29), 7272-7277.

Hasan, A., & Sayigh, A. A. (1994). Some fatty acids as phase-change thermal energy storage materials. *Renewable Energy*, *4*(1), 69-76.

Hasnain, S.M., (1998). Review on sustainable thermal energy storage technologies, Part I: Heat storage materials and techniques. *Energy Conversion & Management,* 39(11):1127-38.

Huang, L., Günther, E., Doetsch, C., & Mehling, H., (2010). Subcooling in PCM emulsions-Part 1: Experimental. *Thermochimica Acta*, 509, 93-99.

Karaipekli, A., & Sarı, A. (2008). Capric–myristic acid/expanded perlite composite as form-stable phase change material for latent heat thermal energy storage. *Renewable Energy*, *33*(12), 2599-2605.

Kousksou, T., Bruel, P., Jamil, A., El Rhafiki, T., & Zeraouli, Y., (2014). Review Energy storage: Applications and challenges. *Solar Energy Materials & Solar Cells*, 120, 59-80.

Li, C., Fu, L., Ouyang, J., & Yang, H. (2013). Enhanced performance and interfacial investigation of mineral-based composite phase change materials for thermal energy storage. *Scientific Reports*, *3*.

Mehling, H., & Cabeza, L. F. (2008). Heat and cold storage with PCM. *Germany*: *Springer Publisher.*

Mehrali, M., Latibari, S. T., Mehrali, M., Indra Mahlia, T. M., Cornelis Metselaar, H. S., Naghavi, et al. (2013). Preparation and characterization of palmitic

acid/graphene nanoplatelets composite with remarkable thermal conductivity as a novel shape-stabilized phase change material. *Applied Thermal Engineering*, *61*(2), 633-640.

Oró, E., De Gracia, A., Castell, A., Farid, M. M., & Cabeza, L. F. (2012). Review on phase change materials (PCMs) for cold thermal energy storage applications. *Applied Energy*, *99*, 513-533.

Sari, A., (2003). Thermal characteristics of a eutectic mixture of myristic and palmitic acids as phase change material for heating applications. *Applied Thermal Engineering*, 23(8) 1005-1017.

Sari, A., Kara, A., & Kaygusuz, K. (2008). Fatty acid/expanded graphite composites as phase change material for latent heat thermal energy storage.*Energy Sources, Part A*, *30*(5), 464-474.

Sari A., Karaipekli, A., & Alkan, C,. (2009). Preparation, characterization and thermal properties of lauric acid/expanded perlite as novel form-stable composite phase change material. *Chemical Engineering Journal*, 155(3) 899-904.

Sarı, A., & Karaipekli, A. (2009). Preparation, thermal properties and thermal reliability of palmitic acid/expanded graphite composite as form-stable PCM for thermal energy storage. *Solar Energy Materials and Solar Cells*, *93*(5), 571-576.

Sari, A., & Karaipekli, A., (2012). Fatty acid esters-based composite phase change materials for thermal energy storage in buildings. *Applied Thermal Engineering*, 37, 208-216.

Sari, A., Karlı, A., Alkan, C., & Karaipekli, A. (2013). Polyethyl Methacrylate (PEMA)/Fatty Acids Blends as Novel Phase Change Materials for Thermal Energy Storage. *Energy Sources, Part A: Recovery, Utilization, and Environmental Effects*, *35*(19), 1813-1819.

Sharma, S. D., & Sagara, K. (2005). Latent heat storage materials and systems: a review. *International Journal of Green Energy*, *2*(1), 1-56.

Sharma, A., Tyagi, V.V., Chen, C.R., & Buddhi, D., (2009). Review on thermal energy storage with phase change materials and applications. *Renewable and Sustainable Energy Reviews*, 13(2) 318-345.

Sheth Karathia, F. (2011). *Analysis of thermal properties of phase change materials (PCM) using differential scanning calorimeter (DSC).* Master Thesis, University of Lleida.

Streicher, W., Cabeza, L., & Heinz, A. (2005). Inventory of Phase Change Materials (PCM). *IEA Solar Heating and Cooling programme-Task*, *32*.

Tavman, I., & Turgut, A., (2010). An investigation on thermal conductivity and viscosity of water based nanofluids. *Microfluidics Based Microsystems*, 139-162.

Turgut, A., Sauter, C., Chirtoc, M., Henry, J.F., Tavman, S., Tavman, I., & Pelzl, J., (2008). AC hot wire measurement of thermophysical properties of nanofluids with 3ω method. *European Physical Journal Special Topics*, 153(1) 349-352.

Yang, X., Yuan, Y., Zhang, N., Cao, X., & Liu, C., (2014). Preparation and properties of myristic–palmitic–stearic acid/expanded graphite composites as phase change materials for energy storage. *Solar Energy,* 99, 259-266.

Wang, C., Feng, L., Li, W., Zheng, J., Tian, W., & Li, X., (2012). Shape-stabilized phase change materials based on polyethylene glycol/porous carbon composite: The influence of the pore structure of the carbon materials. *Solar Energy Materials & Solar Cells*, 105, 21-26.

Wang, X.L., Zhai, X.Q., Wang, T., Wang, H.X., & Yin, Y.L., (2013). Performance of the capric and lauric acid mixture with additives as cold storage materials for high temperature cooling application. *Applied Thermal Engineering*, 58, 252-260.

Wei, T., Zheng, B., Liu, J., Gao, Y., & Guo, W., (2014). Structures and thermal properties of fatty acid/expanded perlitecomposites as form-stable phase change materials. *Energy and Buildings*, 68, 587-592.

Zhang, N., Yuan, Y., Wang, X., Cao, X., Yang, X., & Hu, S., (2013). Preparation and characterization of lauric–myristic–palmitic acid ternary eutectic mixtures/expanded graphite composite phase change material for thermal energy storage. *Chemical Engineering Journal,* 231, 214-219.